

Supporting Information

Intermolecular Coupling and Intramolecular Cyclization of Aryl Nitriles on Au(111)

Henning Klaasen,^{a||} Lacheng Liu,^{bc||} Hong-Ying Gao,^{*bc} Lena Viergutz,^a Philipp A. Held,^a Tobias Knecht,^a Xiangzhi Meng,^{bc} Melanie C. Börner,^{ad} Dennis Barton,^{ade} Saeed Amirjalayer,^{bcd} Johannes Neugebauer,^{ad} Armido Studer^{*a} and Harald Fuchs,^{*bc}

a. Organisch-Chemisches Institut, Westfälische Wilhelms-Universität Münster, Corrensstraße 40, 48149 Münster, Germany. E-Mail: studer@wwu.de

b. Center for Nanotechnology (CeNTech), Heisenbergstraße 11, 48149 Münster, Germany. E-mail: gaoh@wwu.de, fuchsh@wwu.de

c. Physikalisches Institut, Westfälische Wilhelms-Universität, Wilhelm-Klemm-Straße 10, 48149 Münster, Germany.

d. Center for Multiscale Theory and Computation, Westfälische Wilhelms-Universität Münster, Corrensstraße 40, 48149 Münster, Germany.

e. Present address: Physics and Materials Science Research Unit, 162 A, Avenue de la Faiëncerie, University of Luxembourg, L-1511 Luxembourg

|| These authors contributed equally to this work.

Contents

- 1. Chemical synthesis**
- 2. Extended analysis of additional STM and DFT results**
- 3. ^1H - and ^{13}C -NMR spectra of new compounds**

1. Chemical synthesis

General part

Reactions containing air- or moisture-sensitive compounds were performed under argon atmosphere in oven-dried glassware using *Schlenk* techniques.

Chemicals were purchased from *ABCR, Acros Organics, Alfa Aesar, Fluka, TCI, Fluorochem* and *Sigma Aldrich* and used as received. Degassed K_2CO_3 solution (2N) was prepared by sonicating K_2CO_3 (13.8 g, 100 mmol) in H_2O (50 ml) for 10 min, 3 subsequent freeze-and-thaw cycles and bubbling argon into the solution for 1 h.

Solvents for extraction or flash chromatography (FC) and NEt_3 were distilled before use. THF was freshly distilled from K, Et_2O from K/Na alloy prior use and CH_2Cl_2 from P_2O_5 . Dry EtOH, DMF, MeOH and toluene were purchased from *Acros Organics* (Extra Dry over Molecular Sieve, AcroSeal).

Flash chromatography was performed on *Merck* silica gel 60 (40-63 μm) or *Acros Organics* silica gel (35-70 μm) with an excess argon pressure up to 0.5 bar applied. *Merck* silica gel 60 F254 plates were used for thin layer chromatography (TLC) using UV light (254/366 nm) for detection.

1H -NMR (300 MHz and 500 MHz) and **^{13}C -NMR** (75 MHz and 126 MHz) measurements were carried out on a *Bruker DPX 300* and an *Agilent DD2 500* spectrometer respectively. The chemical shifts were referred to the solvent residual peak (1H : $\delta = 7.26$ ppm, ^{13}C : $\delta = 77.16$ ppm ($CDCl_3$) or 1H : $\delta = 2.50$ ppm, ^{13}C : $\delta = 39.52$ ppm ($DMSO-d_6$)). The multiplicity was described as *s* (singlet), *d* (doublet), *t* (triplet), *br* (broad), and *m* (multiplet) as well as its combinations.

All melting points (**MP**) were determined by a *Stuart SMP10* and are uncorrected.

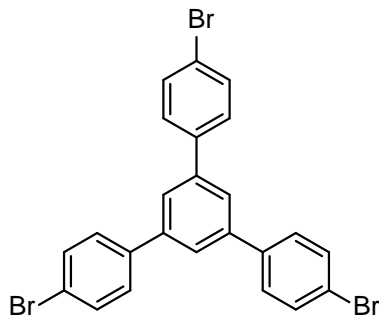
Infrared spectra (**IR**) were recorded by a *Digilab 3100 FT-IR Excalibur Series* spectrometer. The IR signals are listed as *s* (strong), *m* (medium) and *w* (weak) in cm^{-1} .

HR-ESI-MS (m/z) spectra were measured on a *Bruker MicroTof*, **HR-APCI-MS** (m/z) spectra were measured on a *Thermo Fisher Scientific Orbitrap LTQ XL* and **EI-MS** (m/z) spectra were measured on a *Thermo Fisher Scientific TSQ 7000*.

General procedure for Suzuki-coupling of aryl boronic acid with aryl halides (GP1)

The aryl halide (1.00 eq.), the according aryl boronic acid (1.0-3.0 eq.) and Pd(PPh₃)₄ (8.0-8.1 mol%) were dissolved in THF (0.5-30 ml) and aqueous K₂CO₃ solution (2 M, 0.05-2.5 ml) was added dropwise. The reaction mixture was stirred at 80 °C for 24-72 h: After cooling to RT it was added to water and the aqueous layer was extracted with CH₂Cl₂ (3x). The combined organic layers were washed with brine and dried over MgSO₄. After removing the solvents *in vacuo*, the crude product was purified by FC or recrystallization.

1,3,5-Tris(4-bromophenyl)benzene (7)

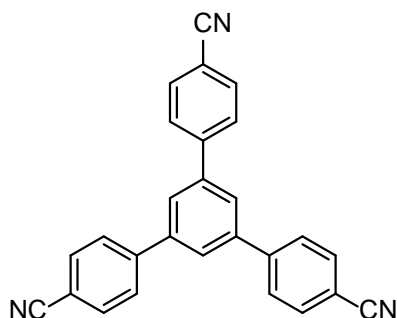


According to a procedure reported in the literature,¹ 4'-bromoacetophenone (3.98 g, 20.0 mmol, 1.00 eq.) was dissolved in ethanol (6 ml) and SOCl₂ (2.40 ml, 33.0 mmol, 1.64 eq.) was added dropwise while stirring. The resulting mixture was stirred at 70 °C for 2 h. After cooling to RT and the addition of saturated aqueous NaHCO₃ solution (50 ml), the precipitate was isolated and washed with water (20 ml) and ethanol (20 ml). The purification by FC (pentane/CH₂Cl₂ 10:1) yielded triphenylbenzene **7** as a pale yellow solid (578 mg, 1.06 mmol, 16%).

¹H NMR (300 MHz, CDCl₃, 293 K): δ = 7.69 (s, 3H, Aryl-H), 7.61 (d, J = 8.5 Hz, 6H, Aryl-H), 7.53 (d, J = 8.5 Hz, 6H, Aryl-H). ¹³C NMR (75 MHz, CDCl₃, 293 K): δ = 141.7 (C), 139.8 (C), 132.2 (CH), 129.0 (CH), 125.1 (CH), 122.3 (C). MS (EI): m/z = {546.6 (8), 545.7 (28), 544.9 (14), 543.7 (100), 542.7 (16), 541.7 (91), 540.8 (3), 539.8 (26)} [M]⁺, {157.9 (0.1), 156.9 (2), 156.2 (0.2), 154.9 (3)}.

Spectroscopic data are in accordance with those described in the literature.¹

1,3,5-Tris(4-cyanophenyl)benzene (1)

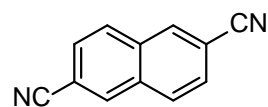


According to a procedure reported in the literature,² 1,3,5-tris(4-bromophenyl)benzene **7** (355 mg, 654 μmol, 1.00 eq.) and CuCN (198 mg, 2.21 mmol, 3.38 eq.) in DMF (3.5 ml) were heated at 155 °C for 25 h under an atmosphere of argon. After cooling the mixture to 90 °C, ethylenediamine (1.5 ml) and water (10 ml) were added and the mixture was extracted with CH₂Cl₂ (3x25 ml). The combined organic layers were dried over MgSO₄ and the solvent was removed *in vacuo*. The purification by FC (CH₂Cl₂) yielded triphenylbenzene **TPB 1** as a white solid (208 mg, 545 μmol, 83%).

¹H NMR (300 MHz, CDCl₃, 293 K): δ = 7.81 (s, 3H, Aryl-H), 7.80-7.78 (m, 12H, Aryl-H). **¹³C NMR** (75 MHz, CDCl₃, 293 K): δ = 144.7 (C), 141.4 (C), 133.0 (CH), 128.1 (CH), 126.5 (CH), 118.7 (C), 112.2 (C). **HRMS** (ESI): m/z calculated for [M+Na]⁺: 404.1158; found: 404.1153.

Spectroscopic data are in accordance with those described in the literature.²

2,6-Dicyanonaphthalene (8)

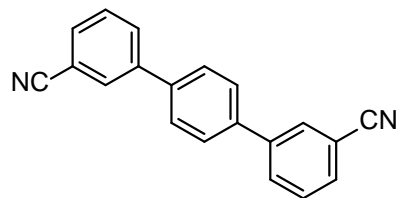


Based on a procedure reported in the literature,² 2,6-dibromonaphthalene (186 mg, 650 μmol, 1.00 eq.) and CuCN (131 mg, 1.46 mmol, 2.25 eq.) in DMF (3.5 ml) were heated at 155 °C for 25 h under an atmosphere of argon. After cooling the mixture to 90 °C, ethylenediamine (1.5 ml) and water (10 ml) were added and the mixture was extracted with CH₂Cl₂ (3x20 ml). The combined organic layers were dried over MgSO₄ and the solvent was removed *in vacuo*. The purification by FC (CH₂Cl₂) yielded dinitrile **8** as a white solid (105 mg, 589 μmol, 91%).

¹H NMR (300 MHz, CDCl₃, 293 K): δ = 8.31-8.28 (m, 2H, Aryl-H), 8.02 (d, *J* = 8.5 Hz, 2H, Aryl-H), 7.76 (dd, *J* = 8.5 Hz, 1.3 Hz, 2H, Aryl-H). **HRMS** (ESI): m/z calculated for [M+Na]⁺: 201.0423; found: 201.0433.

Spectroscopic data are in accordance with those described in the literature.³

p-Terphenyl-3,3''-dicarbonitril (9)

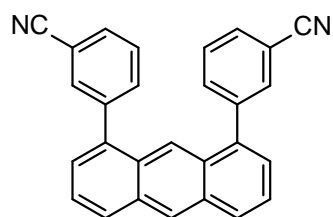


According to **GPI** with 1,4-diiodobenzene (166 mg, 503 μmol, 1.00 eq.), 3-cyanophenylboronic acid (0.22 g, 1.5 mmol, 3.0 eq.) and Pd(PPh₃)₄ (47 mg, 41 μmol, 8.1 mol%) in THF (30 ml) and aqueous K₂CO₃ solution (2 M, 2.5 ml) at 80 °C for 70 h. FC (CH₂Cl₂:pentane 2:1) yielded dinitrile **9** as a colorless solid (114 mg, 407 μmol, 81%).

¹H NMR (300 MHz, CDCl₃, 293 K): δ = 7.92 (dd, *J* = *J* = 1.5 Hz, 2H, Aryl-H), 7.87 (ddd, *J* = *J* = 7.7 Hz, *J* = 1.5 Hz, 2H, Aryl-H), 7.71-7.64 (m, 6H, Aryl-H), 7.58 (dd, *J* = *J* = 7.7 Hz, 2H, Aryl-H).

¹³C NMR (75 MHz, CDCl₃, 293 K): δ = 141.7 (C), 139.1 (C), 131.5 (CH), 131.2 (CH), 130.8 (CH), 129.9 (CH), 128.0 (CH), 118.8 (C), 113.4 (C). **HRMS** (ESI): m/z calculated for [M+Na]⁺: 303.0893; found: 303.0905. **IR** (neat): 3069w, 3041w, 2231m, 1812w, 1699w, 1596w, 1578m, 1525w, 1477m, 1435m, 1395m, 1374w, 1322w, 1280w, 1259w, 1177w, 1125w, 1098w, 1055w, 1014w, 972w, 906m, 849m, 843m, 832m, 781s, 734w, 687s, 619m, 594m, 568m, 531m, 513m. **MP.**: 243-244 °C.

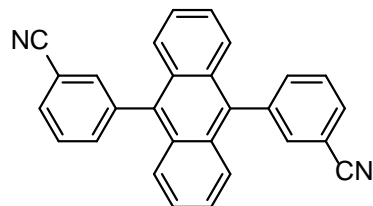
3,3'-(Anthracene-1,8-diyl)dibenzonitrile (10)



According to **GPI** with 1,8-diiodoanthracene (244 mg, 568 μmol, 1.00 eq.), 3-cyanophenylboronic acid (0.25 g, 1.7 mmol, 3.0 eq.) and Pd(PPh₃)₄ (53 mg, 46 μmol, 8.1 mol%) in THF (10 ml) and aqueous K₂CO₃ solution (2 M, 1 ml) at 80 °C for 71 h. FC (pentane:EtOAc 20:1 → 10:1) yielded dinitrile **10** as a colorless solid (202 mg, 531 μmol, 93%).

¹H NMR (300 MHz, CDCl₃, 293 K): δ = 8.59 (*s*, 1H, Aryl-H), 8.23 (*s*, 1H, Aryl-H), 8.09 (*d*, *J* = 8.6 Hz, 2H, Aryl-H), 7.78-7.50 (*m*, 10H, Aryl-H), 7.41 (*dd*, *J* = 6.8 Hz, *J* = 1.2 Hz, 2H, Aryl-H). **¹³C NMR** (75 MHz, CDCl₃, 293 K): δ = 141.7 (C), 138.0 (C), 134.5 (CH), 133.4 (CH), 132.0 (C), 131.2 (CH), 129.9 (C), 129.4 (CH), 128.9 (CH), 127.7 (CH), 127.0 (CH), 125.5 (CH), 122.3 (CH), 118.8 (C), 112.7 (C). **HRMS** (ESI): m/z calculated for [M+Na]⁺: 403.1206; found: 403.1191. **IR** (neat): 3057w, 2957w, 2925s, 2854m, 2362m, 2337w, 2230s, 1734w, 1718w, 1669w, 1653w, 1617w, 1599w, 1576m, 1559w, 1542w, 1526w, 1507w, 1481m, 1437m, 1411w, 1374w, 1322w, 1270m, 1204w, 1179w, 1096w, 909s, 877s, 807s. **MP.**: decomp. >170 °C.

3,3'-(Anthracene-9,10-diyl)dibenzonitrile (11)

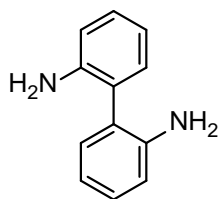


According to **GPI** with 9,10-dibromoanthracene (165 mg, 494 μmol, 1.00 eq.), 3-cyanophenylboronic acid (0.22 g, 1.5 mmol, 3.0 eq.) and Pd(PPh₃)₄ (46 mg, 41 μmol, 8.1 mol%) in THF (10 ml) and aqueous K₂CO₃ solution (2 M, 1 ml) at 80 °C for 24 h. FC (pentane:EtOAc 20:1 → 8:1) yielded dinitrile **11** as a yellow solid (155 mg, 407 μmol, 82%) as a mixture of diastereomers (dr 1:1).

¹H NMR (300 MHz, CDCl₃, 293 K): δ = 7.93-7.87 (*m*, 2H, Aryl-H), 7.83-7.72 (*m*, 6H, Aryl-H), 7.62-7.51 (*m*, 4H, Aryl-H), 7.47-7.36 (*m*, 4H, Aryl-H). **¹³C NMR** (75 MHz, CDCl₃, 293 K): δ = 140.4 (C), 136.0 (CH), 135.9 (CH), 135.2 (C), 134.8 (CH), 134.8 (CH), 131.6 (C), 129.8 (C), 129.7 (CH), 129.6 (CH), 126.4 (CH), 126.1 (CH), 118.8 (C), 118.7 (C), 113.2 (C), 113.2 (C). **HRMS** (ESI): *m/z* calculated for [M+Na]⁺: 403.1206; found: 403.1218. **IR** (neat): 3065w, 2925m, 2855w, 2362m, 2337m, 2231s, 1718w, 1685w, 1653w, 1599m, 1576m, 1559w, 121w, 1482m, 1457w, 1441s, 1386s, 1218w, 1171w, 1096w, 1029m, 1029m, 999w, 974w, 911s, 830m. **MP.**: decomp. >234 °C.

While the ¹H NMR signals of both diastereomers overlay, some of the ¹³C NMR signals differ, which explains the overrepresented signals. High temperature NMR studies indicated that these signals are due to the presence of two diastereomers.

2,2'-Diaminobiphenyl (**12**)

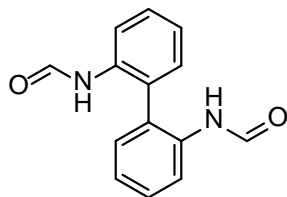


To a solution of 2,2'-dinitrobiphenyl (1.00 g, 4.09 mmol, 1.00 eq.) in MeOH (50 ml) Pd/C (0.44 g, 0.41 mmol, 10 mol%) was added and the mixture was stirred under an atmosphere of hydrogen for 23 h at RT. After filtration through a pad of celite, the solvent was removed *in vacuo*. FC (EtOAc:pentane:NEt₃ 1:1:0.01) yielded diamine **12** as a yellow solid (627 mg, 3.40 mmol, 83%).

¹H NMR (300 MHz, CDCl₃, 293 K): δ = 7.34–7.02 (*m*, 4H, Aryl-H), 7.02–6.63 (*m*, 4H, Aryl-H), 3.69 (*brs*, 4H, NH₂). **¹³C NMR** (75 MHz, CDCl₃, 293 K): δ = 144.2 (C), 131.1 (CH), 128.8 (CH), 124.6 (C), 118.8 (CH), 115.6 (CH). **HRMS** (ESI): *m/z* calculated for [M+Na]⁺: 185.1073, found: 185.1084.

Spectroscopic data are in accordance with those described in the literature.⁴

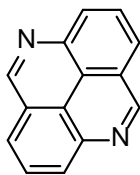
N,N'-(Biphenyl-2,2'-diyl)diformamid (**13**)



Based on procedures reported in the literature,^{5,6} acetic anhydride (1.5 ml, 16 mmol, 5.0 eq.) was added to formic acid (0.60 ml, 16 mmol, 5.0 eq.) and the mixture was stirred at 55 °C for 2 h. The reaction mixture was then added dropwise to a solution of diamine **12** (585 mg, 3.18 mmol, 1.00 eq.) in THF (10 ml) at 0 °C. After warming to RT, stirring was continued for 2 h. Afterwards the reaction was quenched by addition of saturated aqueous NaHCO₃-Lösung (20 ml). The aqueous layer was extracted with EtOAc (3x30 ml) and the combined organic layers were dried over MgSO₄. After removing the solvent *in vacuo*, the crude product of **13** was used for the next reaction step without further purification.

HRMS (ESI): *m/z* calculated for [M+Na]⁺: 263.0791, gefunden: 263.0802.

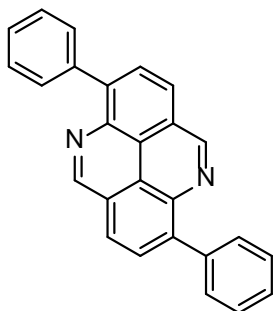
4,9-Diazapyrene (**14**)



According to a procedure reported in the literature⁷ crude **13** was added to a molten mixture of NaCl (2.98 g, 50.9 mmol, 16.0 eq.) and AlCl₃ (13.6 g, 102 mmol, 32.0 eq.) at 100 °C. The mixture was stirred at 230 °C for 8 h. After cooling to RT the mixture was added to an ice/water mixture (50 ml). The mixture was alkalinized and extracted with toluene (2x100 ml). The combined organic layers were washed with brine (50 ml) and dried over MgSO₄. After removing the solvent *in vacuo*, FC (EtOAc:pentane 2:1→3:1→4:1) yielded diazapyrene **14** as an orange solid (393 mg, 1.92 mmol, 61% over two steps).

¹H NMR (300 MHz, CDCl₃, 293 K): δ = 9.70 (s, 2H, Aryl-H), 8.66 (dd, *J* = 7.9, 1.0 Hz, 2H, Aryl-H), 8.40 (dd, *J* = 7.7 Hz, 1.0 Hz, 2H, Aryl-H), 8.26 (dd, *J* = 7.8 Hz, 2H, Aryl-H). **¹³C NMR** (75 MHz, CDCl₃, 293 K): δ = 154.5 (CH), 141.9 (C), 130.0 (CH), 128.8 (CH), 125.5 (CH), 125.2 (C), 120.4 (C). **HRMS** (ESI): *m/z* calculated for [M+H]⁺: 205.0766, found: 205.0745. **IR** (neat): 3368s, 2362m, 2335m, 1684w, 1653w, 1572w, 1475s, 1253m, 937w, 841w, 789s, 718m, 691m. **MP.**: 211-214 °C.

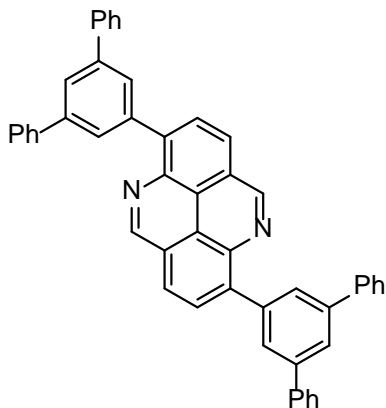
4,9-Diaza-3,8-diphenylpyrene (3)



Based on a procedure reported in the literature⁸ 4,9-diazapyrene **14** (122 mg, 598 μmol , 1.00 eq.) and 1,3-dimesitylimidazolium chloride (IMes•HCl, 24.5 mg, 71.9 μmol , 12.0 mol%) were added to an oven-dried schlenk tube and brought into an Ar filled glovebox. $\text{Rh}_2(\text{OAc})_4$ (15.9 mg, 36.0 μmol , 6.01 mol%) and NaOtBu (144 mg, 1.50 mmol, 2.51 eq.) were added to the schlenk tube and taken outside the box. Afterwards, toluene (0.6 ml) and bromobenzene (124 μL , 1.18 mmol, 1.98 eq.) were transferred into the tube under a positive stream of Ar and the reaction mixture was stirred vigorously for 24 h at 95 °C. After removing the solvent *in vacuo*, FC (EtOAc:pentane 1:2→2:1→3:1) and several recrystallizations (toluene) yielded diazapyrene **DP 3** as an orange solid (30 mg, 84 μmol , 14%).

¹H NMR (300 MHz, CDCl_3 , 293 K): δ = 9.73 (*s*, 2H, Aryl-H), 8.43 (*d*, J = 8.0 Hz, 2H, Aryl-H), 8.32 (*d*, J = 7.9 Hz, 2H, Aryl-H), 7.93-7.90 (*m*, 4H, Aryl-H), 7.64-7.58 (*m*, 4H, Aryl-H), 7.54-7.48 (*m*, 2H, Aryl-H). **¹³C NMR** (75 MHz, CDCl_3 , 293 K): δ = 154.3 (CH), 141.9 (C), 139.5 (C), 139.3 (C), 131.3 (CH), 130.6 (CH), 128.5 (CH), 128.2 (CH), 125.2 (CH), 124.7 (C), 121.7 (C). **HRMS** (ESI): m/z calculated for $[\text{M}+\text{H}]^+$: 357.1386, found 357.1387. **IR** (neat): 2958m, 2925s, 2854m, 2160w, 1672w, 1579w, 1477s, 1223w, 1012w, 991w, 910w, 827w, 774s, 730m, 693s. **MP.**: decomp. >268 °C

4,9-Diaza-3,8-bis(3,5-phenylphen-1-yl)pyrene (4)

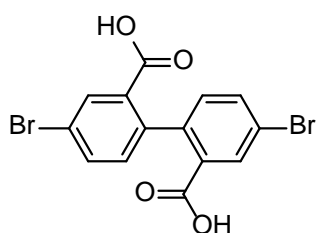


Based on a procedure reported in the literature,⁸ 4,9-diazapyrene **14** (82 mg, 0.40 mmol, 1.0 eq.), 5'-bromo-1,1':3,1''-terphenyl (247 mg, 799 μmol , 1.99 eq.) and IMes•HCl (16.4 mg, 48.1 μmol , 12.0 mol%) were added to an oven-dried schlenk tube and brought into an Ar filled glovebox. $\text{Rh}_2(\text{OAc})_4$ (10.6 mg, 24.0 μmol , 5.97 mol%) and NaOtBu (96.1 mg, 1.00 mmol, 2.49 eq.) were added to the schlenk tube and taken outside the box. Afterwards, toluene (0.4 ml) was transferred into the tube under a positive stream of Ar and the reaction mixture was stirred vigorously for 24 h at 95 °C. The reaction mixture was then cooled to RT and filtrated

through a silica pad. After removing the solvent *in vacuo*, FC (EtOAc:pentane 0:1→1:20) yielded diazapyrene **DAP 4** as an orange solid (45 mg, 68 μ mol, 17%).

^1H NMR (300 MHz, CDCl_3 , 293 K): δ = 9.76 (*s*, 2H, Aryl-H), 8.51-8.38 (*m*, 4H, Aryl-H), 8.14 (*s*, 4H, Aryl-H), 7.97 (*s*, 2H, Aryl-H), 7.80 (*d*, J = 7.3 Hz, 8H, Aryl-H), 7.51 (*m*, 8H, Aryl-H), 7.41 (*m*, 4H, Aryl-H). **^{13}C NMR** (75 MHz, CDCl_3 , 293 K): δ = 154.4 (CH), 141.9 (C), 141.7 (C), 141.4 (C), 140.1 (C), 139.6 (C), 130.6 (CH), 129.3 (CH), 129.0 (CH), 127.7 (CH), 127.7 (CH), 126.1 (CH), 125.3 (CH), 124.8 (C), 121.6 (C). **HRMS** (ESI): m/z calculated for $[\text{M}+\text{H}]^+$: 661.2638, found 661.2616. **IR** (neat): 3056w, 3032w, 2926w, 2885w, 1653w, 1594m, 1576m, 1485m, 1465m, 1424w, 1411w, 1353w, 1286w, 1248w, 1223w, 1189w, 1156w, 1127w, 1075w, 1031w, 995w, 934w, 907m, 881m, 827m, 757s, 730m, 696m. **MP.**: decomp. >235 $^\circ\text{C}$.

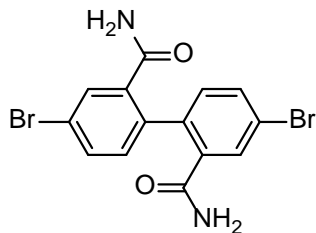
4,4'-Dibromobiphenyl-2,2'-dicarboxylic acid (**15**)



Based on a procedure reported in the literature,⁹ diphenic acid (1.45 g, 6.00 mmol, 1.00 eq.) was dissolved in concentrated H_2SO_4 (18 ml) and cooled to 0 $^\circ\text{C}$. Dibromoisocyanuric acid (1.76 g, 6.13 mmol, 1.02 eq.) was added in portions and the resulting mixture was stirred at RT for 18 h. Afterwards it was added to ice water (180 ml). The precipitate was filtrated, washed with water (2x30 ml) and pentane (2x 10 ml). After drying the crude product **15** under HV it was used for the next step without further purification.

HRMS (ESI): m/z calculated for $[\text{M}-\text{H}]^-$: 396.87166, found: 396.87129.

4,4'-Dibromobiphenyl-2,2'-dicarboxamide (**16**)

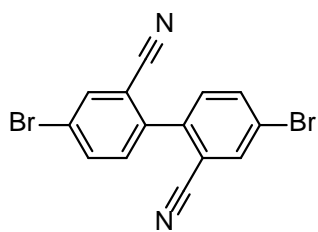


Crude **15** was dissolved in SOCl_2 (6 ml) and stirred at reflux for 2 h. After cooling to RT, volatiles were removed under HV. The residue was treated with toluene (6 mL) and aqueous NH_3 (28%, 6 ml) was added dropwise at 0 $^\circ\text{C}$. The resulting mixture was stirred at RT for 2 h. Afterwards aqueous HCl (1 M, 10 ml) was added and the aqueous layer was extracted with EtOAc

(3x50 ml). The combined organic layers were dried over MgSO₄ and the solvents were removed *in vacuo*. FC (EtOAc:pentane 3:1) yielded diamide **16** as a yellow solid (960 mg, 2.41 mmol, 40%).

¹H NMR (300 MHz, DMSO-*d*₆, 293 K): δ = 7.98 (*s*, 2H, CONH₂), 7.69-7.61 (*m*, 4H, Aryl-H), 7.47 (*s*, 2H, CONH₂), 7.04 (*d*, *J* = 8.0 Hz, 2H, Aryl-H). ¹³C NMR (75 MHz, DMSO-*d*₆, 293 K): δ = 169.1 (CONH₂), 138.5 (C), 136.7 (C), 131.9 (CH), 131.2 (CH), 129.7 (CH), 120.8 (C). HRMS (ESI): *m/z* calculated for [M+Na]⁺: 418.90012, found: 418.90002. IR (neat): 3319w, 3170w, 1729w, 1661s, 1610m, 1582m, 1553w, 1466w, 1411m, 1372m, 1253w, 1157w, 1085w, 1045w, 1004m, 894w, 824w. MP: decomp. >207 °C.

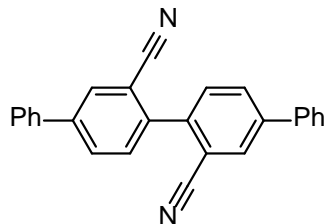
4,4'-Dibromobiphenyl-2,2'-dicyanitrile (**17**)



Diamide **16** (958 mg, 2.41 mmol, 1.00 eq.) was dissolved in CH₂Cl₂ (25 ml) and NEt₃ (5.3 ml, 38 mmol, 16 eq.) was added at 0 °C. After the dropwise addition of TFAA (3.3 ml, 24 mmol, 9.8 eq.) the resulting mixture was allowed to warm to RT and then stirred at this temperature for 25 h. The reaction was quenched upon addition of H₂O (50 ml) and EtOAc (100 ml). The phases were separated and the organic layer was washed with saturated aqueous NaHCO₃ (100 ml) and dried over MgSO₄. Recrystallization (CH₂Cl₂/pentane) yielded dinitrile **17** as a yellow solid (149 mg, 412 μ mol, 17%).

¹H NMR (300 MHz, CDCl₃, 293 K): δ = 7.96 (*d*, *J* = 2.0 Hz, 2H, Aryl-H), 7.86 (*dd*, *J* = 8.4, 2.0 Hz, 2H, Aryl-H), 7.43 (*d*, *J* = 8.4 Hz, 2H, Aryl-H). ¹³C NMR (75 MHz, CDCl₃, 293 K): δ = 139.4 (C), 136.5 (CH), 136.3 (CH), 131.9 (CH), 123.8 (C), 116.1 (C), 114.2 (C). HRMS (ESI): *m/z* calculated for [M+Na]⁺: 382.8790, found: 382.8792. IR (neat): 2963w, 2928w, 2232w, 2201w, 2163w, 2009m, 1972w, 1584w, 1465m, 1260s, 1187w, 1091s, 1018s, 903w, 821s, 805s. MP: 250-252 °C

[1,1':4',1'':4'',1''':4''']-Quarterphenyl]-2'',3'-dicyanitrile (5)

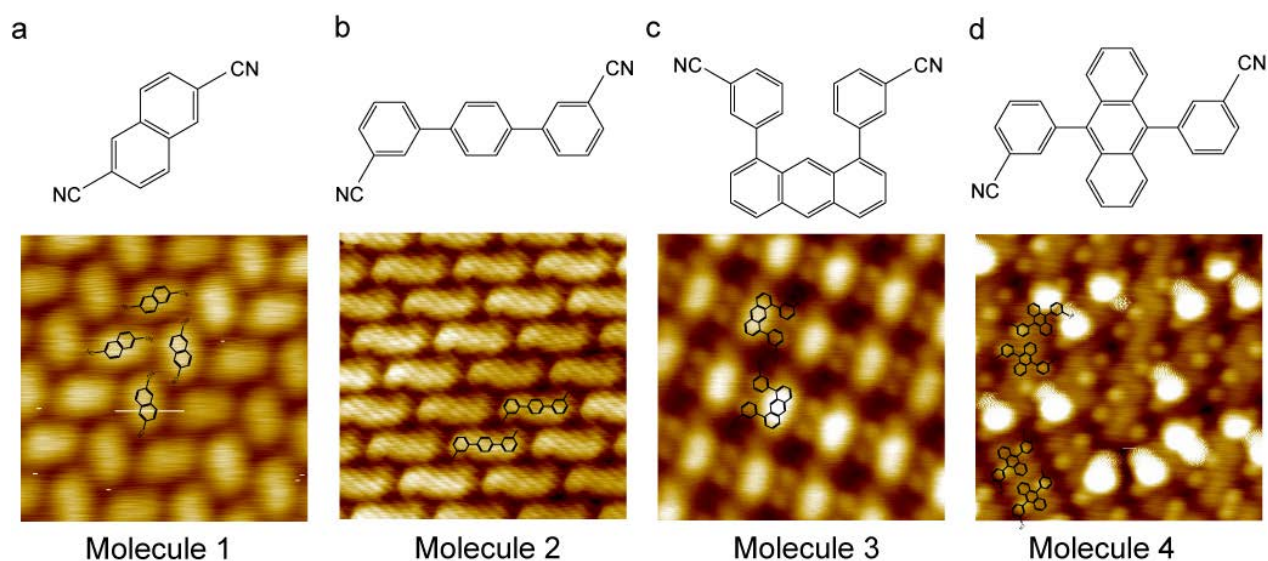


According to **GPI** with dinitrile **17** (109 mg, 301 μmol , 1.00 eq.), phenylboronic acid (110 g, 902 μmol , 3.00 eq.) and $\text{Pd}(\text{PPh}_3)_4$ (28 mg, 24 μmol , 8.0 mol%) in THF (1 ml) and aqueous K_2CO_3 solution (2 M, 0.10 ml) at 80 °C for 69 h. Instead of CH_2Cl_2 , CHCl_3 (6x5 ml) was used for extraction and recrystallization (CH_2Cl_2 :pentane) yielded **QDN 5** as a colorless solid (104 mg, 292 μmol , 97%).

$^1\text{H NMR}$ (500 MHz, CDCl_3 , 293 K): δ = 8.05 (*d*, J = 2.0 Hz, 2H, Aryl-H), 7.94 (*dd*, J = 8.2, 2.0 Hz, 2H, Aryl-H), 7.71 (*d*, J = 8.2 Hz, 2H, Aryl-H), 7.67-7.62 (*m*, 4H, Aryl-H), 7.56-7.42 (*m*, 6H, Aryl-H). $^{13}\text{C NMR}$ (126 MHz, CDCl_3 , 293 K): δ = 142.7 (C), 139.9 (C), 138.3 (C), 132.3 (CH), 131.6 (CH), 131.3 (CH), 129.4 (CH), 128.9 (CH), 127.3 (CH), 117.9 (C), 113.0 (C). **HRMS** (ESI): m/z calculated for $[\text{M}+\text{Na}]^+$: 379.1206, found: 379.1206. IR (neat): 2934m, 2923m, 2855w, 2554w, 2416w, 2272m, 2226m, 2159s, 2010m, 1599w, 1473s, 1449w, 1380w, 1301w, 1260w, 1032w, 897w, 843w, 772s, 763s, 699s, 587m. **MP**: >300 °C.

2. Extended analysis of additional STM and DFT results

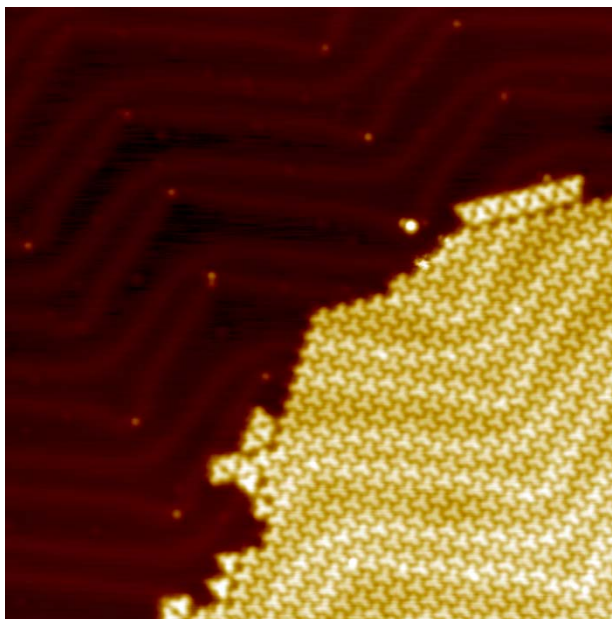
a. Dinitriles measurements.



SI-Figure 1. Overview of various dinitriles we measured at Au(111). (a-d) The upper half shows chemical structures and the lower shows their respective high resolution STM images at Au(111) surface (a, $4 \times 4 \text{ nm}^2$, - 2 V, 50 pA; b, $5 \times 5 \text{ nm}^2$, - 0.5 V, 300 pA; c, $4.4 \times 4.4 \text{ nm}^2$, - 2.5 V, 10 pA; d, $5.8 \times 5.8 \text{ nm}^2$, - 2 V, 10 pA).

It is necessary to point out that all efforts on various dinitriles towards polymerization failed. No covalent coupling of these dinitriles was clearly identified (for all Ag(111), Cu(111) and Au(111) cases), only self-assembly and coordinated chains (for Cu(111) case) were observed.

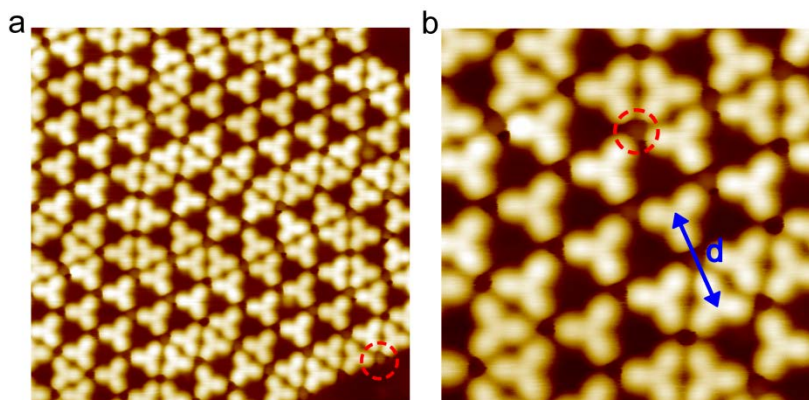
b. Low coverage case of TPB 1 on Au(111) surface



SI-Figure 2. STM image of **TPB 1** deposited on an Au(111) substrate which was at room temperature during the deposition ($42 \times 42 \text{ nm}^2$, -1.5 V , 10 pA). The coverage is much lower than 1 ML (monolayer) controlled by only 20% of the deposition time needed for 1 ML (see manuscript Figure 1a)).

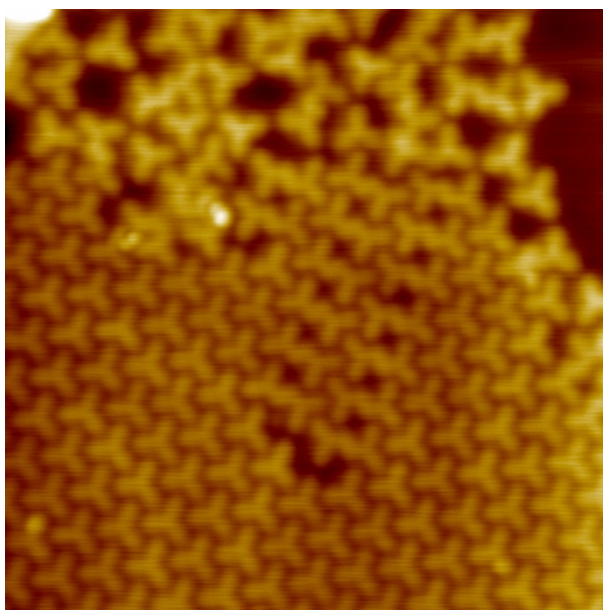
It is shown that **TPB 1** aggregates in big islands with the same self-assembly structure on Au(111) surface for high and low coverage case. No obvious coverage dependency was observed.

c. TPB molecule at Au(111) surface.

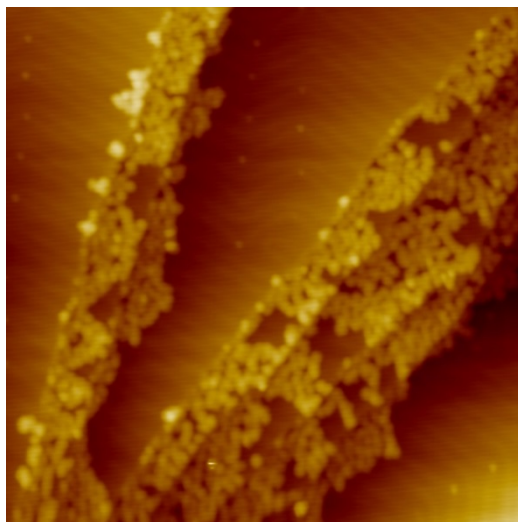


SI-Figure 3. High resolution STM image of the organometallic network. (a). Overview STM image ($16.8 \times 16.8 \text{ nm}^2$, -0.9 V , 200 pA), (b). Zoomed-in STM image ($8.4 \times 8.4 \text{ nm}^2$, -0.9 V , 200 pA). One gold adatom was highlighted by a red circle. The center-to-center distance d is measured to be $2.00 \pm 0.02 \text{ nm}$.

With a specific tip (maybe terminated by one molecule), the gold adatoms can be identified between the organic molecules. This is best visible at the edge of the organometallic network. In case of the dimeric structure no adatoms were clearly observed inside the structure.

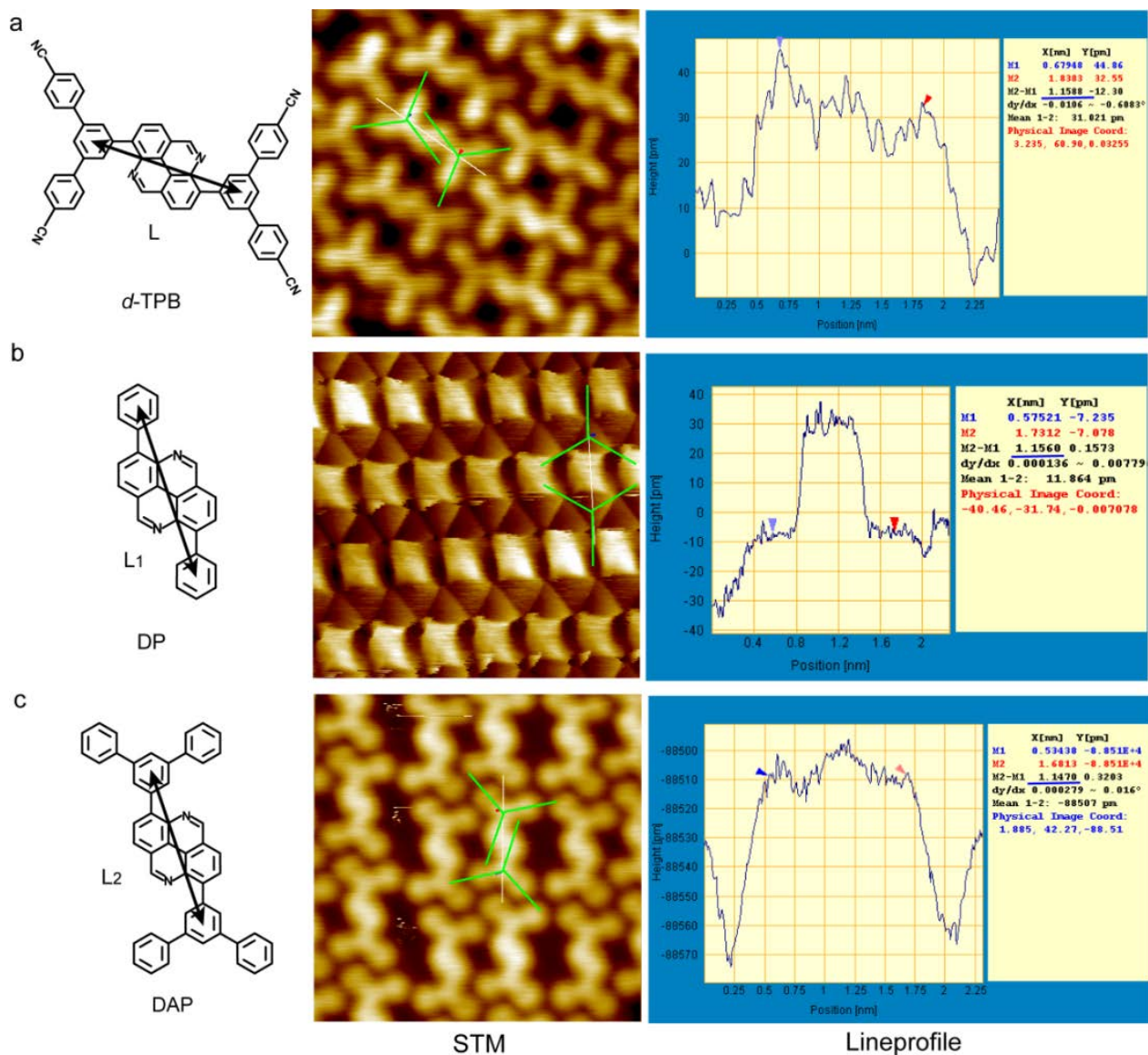


SI-Figure 4. STM image at the edge of a closely packed self-assembled structure after thermal annealing to $240 \text{ }^\circ\text{C}$ ($17 \times 17 \text{ nm}^2$, 0.5 V , 10 pA).



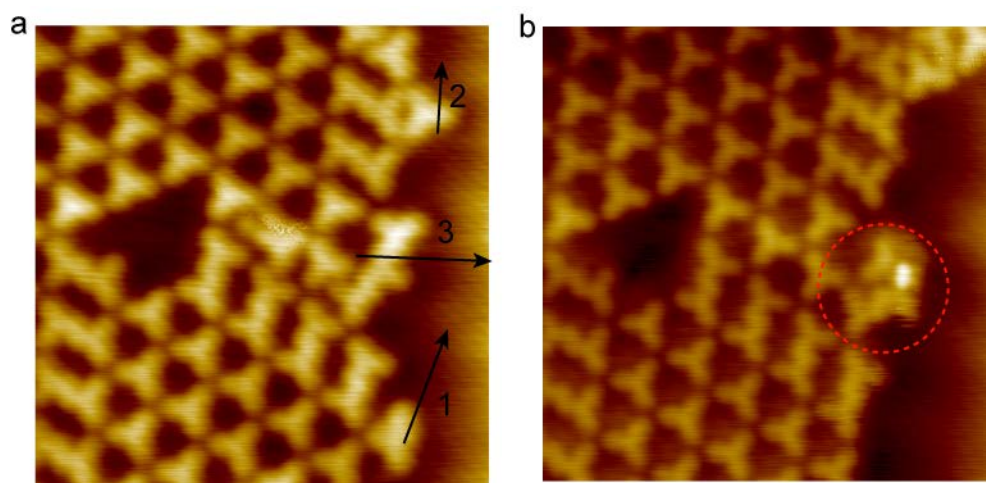
SI-Figure 5. *STM image of the TPB sample after thermal annealing to 283 °C ($84 \times 84 \text{ nm}^2$, 2 V, 10 pA).*

d. Distance measurements, STM manipulations towards *d*-TPB 2.



SI-Figure 6: Distance measurements and lineprofiles of *d*-TPB 2. In (a) and (c), the distance is calculated between former core benzene rings in the TPB along the lineprofile. The former core benzene rings of TPB were calibrated by three intersectant center lines (green) along the feature of the former TPB. Ten different molecules are measured independently. The given length is the average value and the error is the standard error of the mean. In (a), the distance shown here was measured to be 1.16 nm, and the average distance of 10 measurements is 1.16 ± 0.02 nm. In (c), the distance shown here was measured to be 1.15 nm, and the average distance of 10 measurements is 1.15 ± 0.02 nm. However, in (b), the image was obtained by a specific tip without clear feature

of the terminal benzene rings. It is difficult to calibrate the center of the benzene ring. The attached triangular features at the ends of the DP molecules were assigned as the benzene rings and the center was used for distance measurements. The average distance of 10 measurements is 1.16 ± 0.02 nm. The distance $L1$ in DP was measured to show that the distances L , $L1$ and $L2$ are comparable.



SI-Figure 7. STM manipulation towards **d-TPB 2**. (a) Before and (b) after manipulation (acquired at 0.5 V and 1 V, 100 pA, 12.5×12.5 nm², respectively). The directions of manipulation were marked by black arrows.

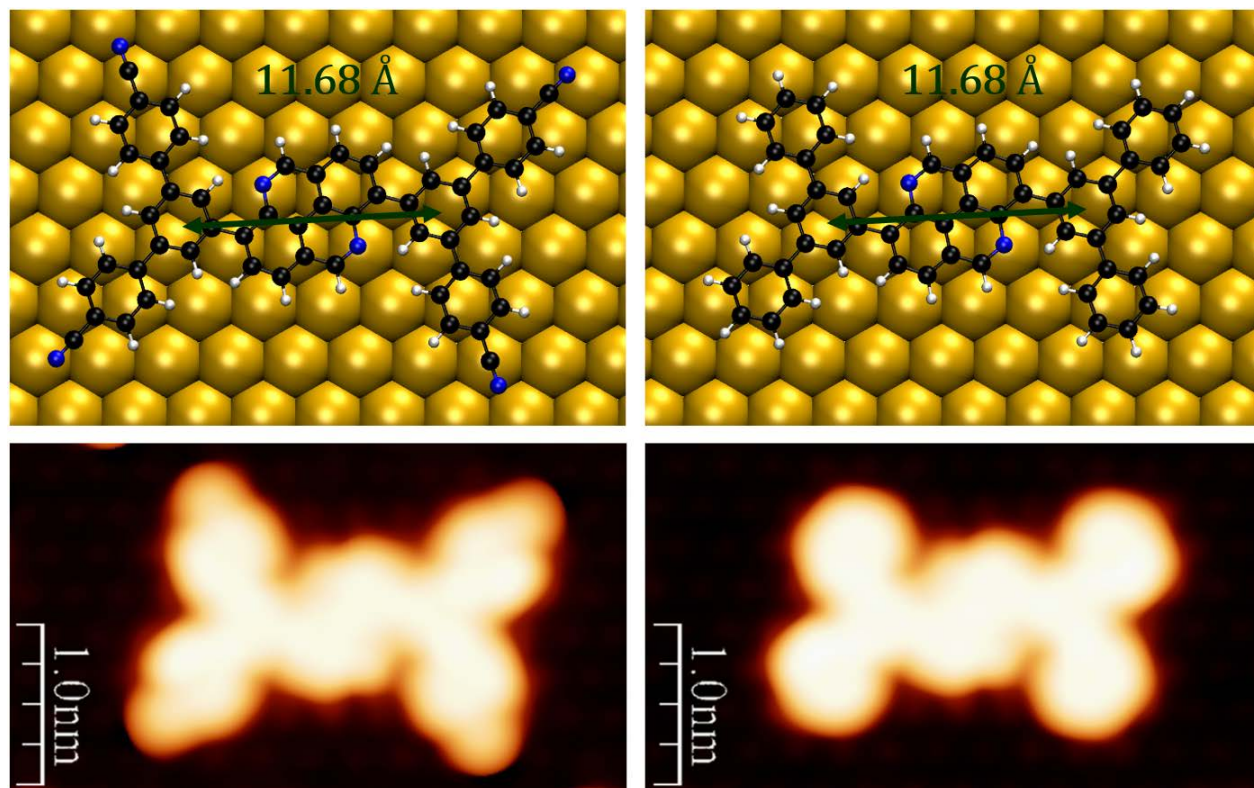
The STM manipulation 1 and 2 were towards the nitrile coordinated **TPB** molecules, which turns out they can be separated from the networks individually. STM manipulation 3 towards to one **TPB** coordinated with one **d-TPB 2** dimer, which turns out that the **d-TPB 2** dimer was rotated as a whole and the nitrile-coordination was bent.

e. Computational details, optimized structures of **d-TPB 2** and **DAP 4** at Au(111) and STM simulation

Computational Details:

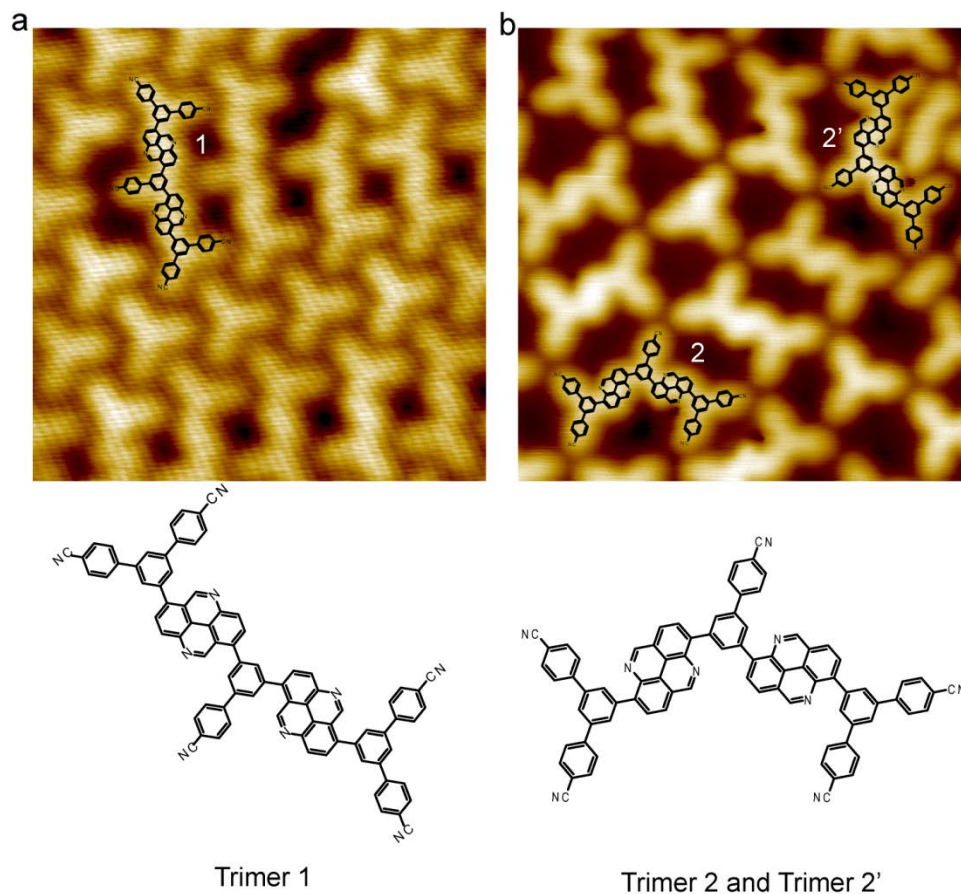
Periodic DFT calculations (surface simulations) were carried out using VASP 5.4.4¹⁰⁻¹² and projector-augmented-wave-based pseudopotentials^{13,14} in the 5.2 PBE variant. To describe

exchange and correlation, the PBE functional was used^{15,16} and long-range dispersion interactions were taken into account by applying the D3 dispersion correction¹⁷ with Becke–Johnson damping.¹⁸⁻²¹ The basis set was limited at an energy cutoff of 500 eV and the k-space was sampled using 1x2x1 k-points. The surface was modeled by a three-layer p(12x8) Au(111) slab with 15 Å vacuum separation based on a calculated lattice constant of 4.10 Å (experimental 4.08 Å²²). During the structural relaxation, the two lowermost layers were kept fixed and the forces were converged to 0.01 eV/Å. A dipole correction along the surface normal was applied. The STM simulations were performed within the Tersoff-Hamann approximation,²³ using the FHI-aims software.²⁴ The converged geometries obtained by the VASP calculations were employed and the same structural parameters as mentioned above were used. While all possible computational parameters were also kept fixed, the 'tier 1/light' basis set and the many-body dispersion energy correction²⁵⁻²⁶ were applied. The images showing the geometries were generated using VMD 1.9.4.²⁷ and the simulated STM images were created with the WSxM²⁸ software.



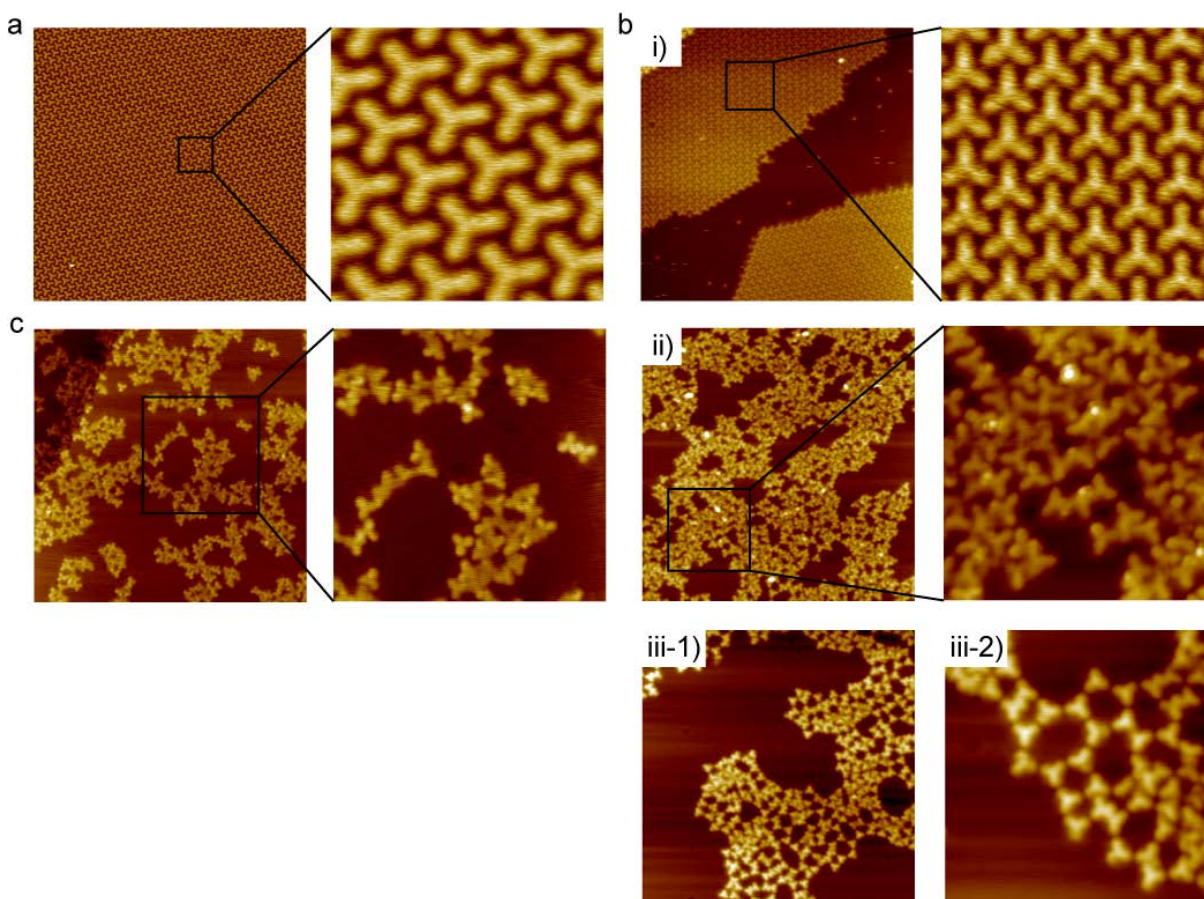
SI-Figure 8. Top: Geometry of *d*-TPB 2 (left) and DAP 4 (right) from converged periodic DFT calculations (starting from the respective gas phase geometries). Bottom: STM simulations of *d*-TPB 2 (left, $U = 0.5$ V) and DAP 4 (right, $U = 0.5$ V).

f. t-TPB at Au(111) surface



SI-Figure 9. Trimers formed by *TPB* on *Au(111)* surface. (a) STM image of trimer 1 ($7 \times 7 \text{ nm}^2$, 0.6 V, 10 pA) and its probable structure sketch. (b) STM image of trimer 2 ($7 \times 7 \text{ nm}^2$, 1 V, 5 pA) and its probable structure sketch, the trimer 2' and trimer 2 are diastereomers at the surface.

g. TPB molecules at Ag(111), Cu(111) and Cu(100) surfaces.

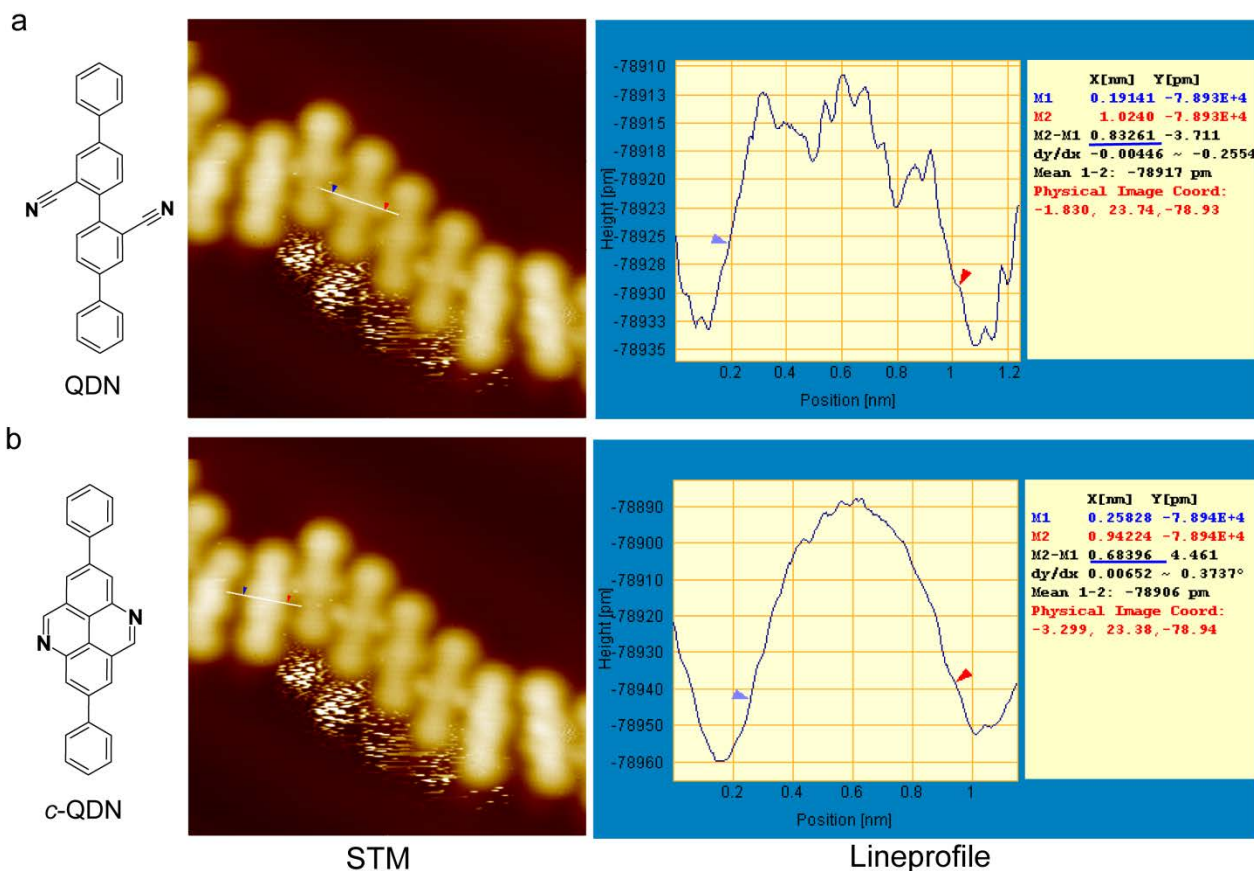


SI-Figure 10. *TPB* molecules at Ag(111), Cu(111) and Cu(100) surfaces. (a) STM images of *TPB* deposition at Ag(111) surface (Overview, $42.1 \times 42.1 \text{ nm}^2$ and zoomed-in, $5 \times 5 \text{ nm}^2$, 0.5 V, 50 pA). (b) STM images of *TPB* at Cu(111) surface. b-i) As grown (overview, $42 \times 42 \text{ nm}^2$ and zoomed-in, $7 \times 7 \text{ nm}^2$, 0.5 V, 5 pA and 10 pA, respectively); b-ii) Annealing at 170 °C (overview, $42 \times 42 \text{ nm}^2$ and zoomed-in, $12 \times 12 \text{ nm}^2$, 0.5 V, 50 pA); b-iii) Hot surface deposition at 185 °C (iii-1, overview, $42 \times 42 \text{ nm}^2$ and high resolution, $16 \times 16 \text{ nm}^2$, 0.5 V, 10 pA). (c) STM images of *TPB* at Cu(100) surface after annealing at 175 °C (overview, $42 \times 42 \text{ nm}^2$ and zoomed-in, $17 \times 17 \text{ nm}^2$, 0.5 V, 50 pA).

At Ag(111) surface, **TPB** will form a self-assembly structure after deposition (SI-Figure 6.a) and desorb after annealing, no reactions were identified. At Cu(111) surface, **TPB** formed the same self-assembly structure after deposition (SI-Figure 6.b-i), and after thermal annealing **TPB** formed various dimer, trimer and tetramer complexes via CN coordination or CN covalent coupling (SI-Figure 6.b-ii). Here, it is not easy to distinguish whether the dimers (especially the nonlinear linked

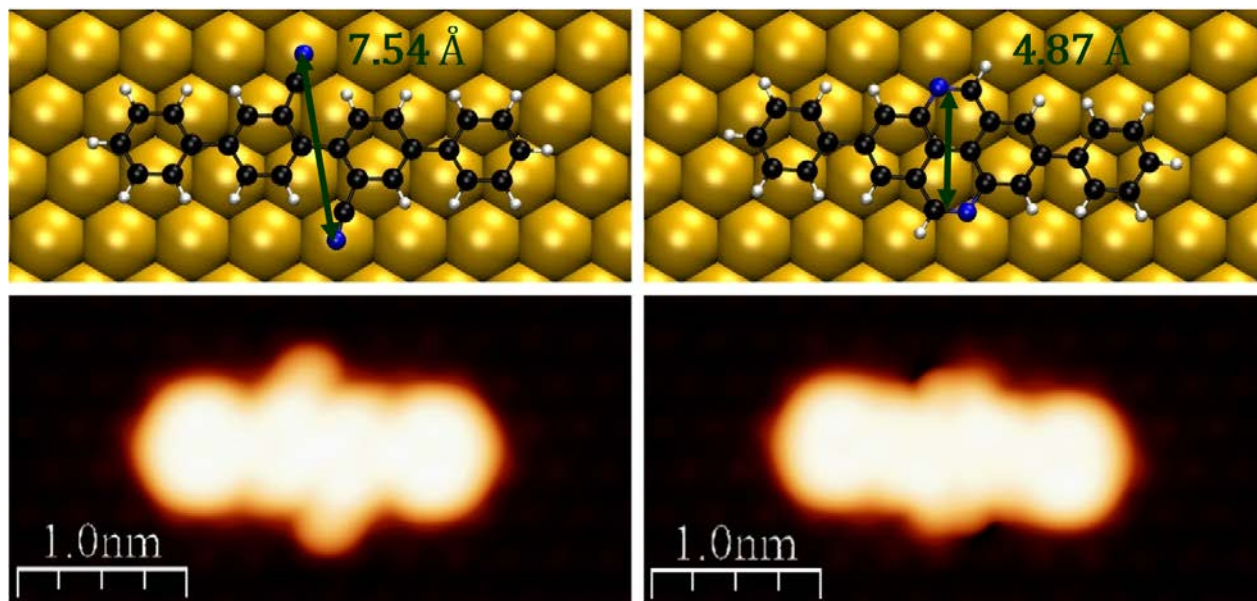
dimers) were linked by CN coordination or CN covalent coupling. Hot surface grow **TPB** slowly, can give better coordinated **TPB** complexes/structures and CN covalent coupling **TPB**-dimers, as compared with the directly annealed sample (SI-Figure 6.b-iii).

h. Distance measurement of QDN before and after the surface reaction as well as lineprofiles.



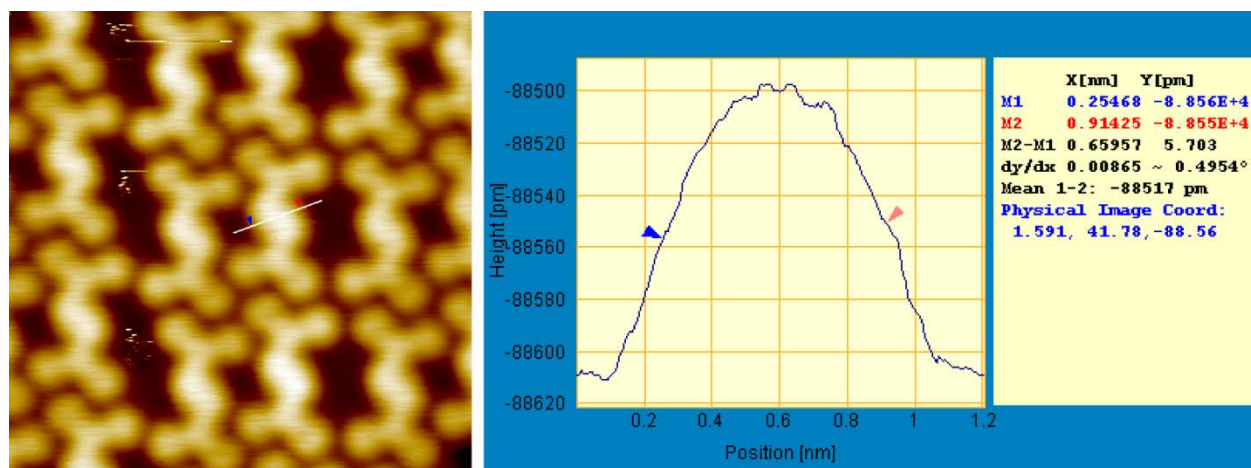
SI-Figure 11. Distance measurements of **QDN** and **c-QDN** on Au(111) after annealing to 215 °C. (a). The edge to edge distance measurement of unreacted **QDN** and its lineprofile along the molecule. The distance shown here is measured to be 0.83 nm, and the average distance of 10 measurements is 0.82 ± 0.02 nm. (b). The edge-to-edge distance measurement of **c-QDN** (after reaction) and its lineprofile along the molecule. The distance showed here is measured to be 0.68 nm, and the average distance of 10 measurements is 0.69 ± 0.02 nm. Please note that the edge-to-edge distances are highly influenced by the STM contrast and do not represent the width of the molecules. As both molecules are in the same STM image with the same contrast, it can still be shown that the distance shrinks dramatically after the reaction.

i. Optimized structures of QDN 5 and *c*-QDN 6 at Au(111) and STM simulation



SI-Figure 12: Top: Geometry of **QDN 5** (left) and ***c*-QDN 6** (right) from converged periodic DFT calculations (starting from the respective gas phase geometries). Bottom: STM simulations of **QDN 5** (left, $U = 0.5$ V) and ***c*-QDN 6** (right $U = 0.5$ V). The distances given in the optimized structures only show the shrinking of the molecule after the reaction. The experimentally measured edge to edge distances are larger than those calculated by DFT because of the enlargement effect by scanning probe microscopy and the influence of the contrast.

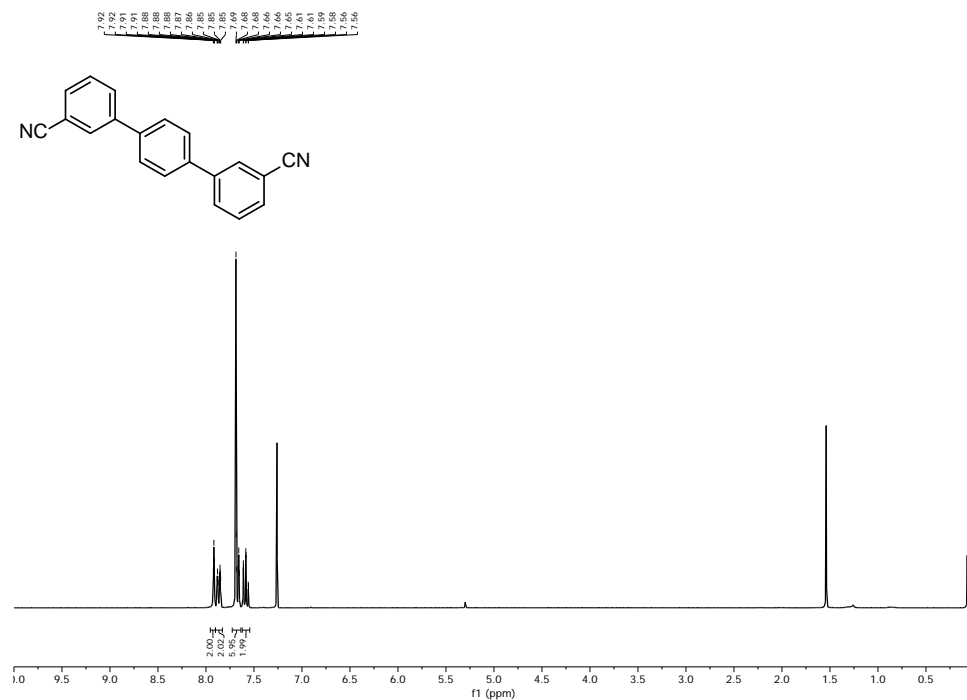
j. Width of DAP 4 measured in STM studies



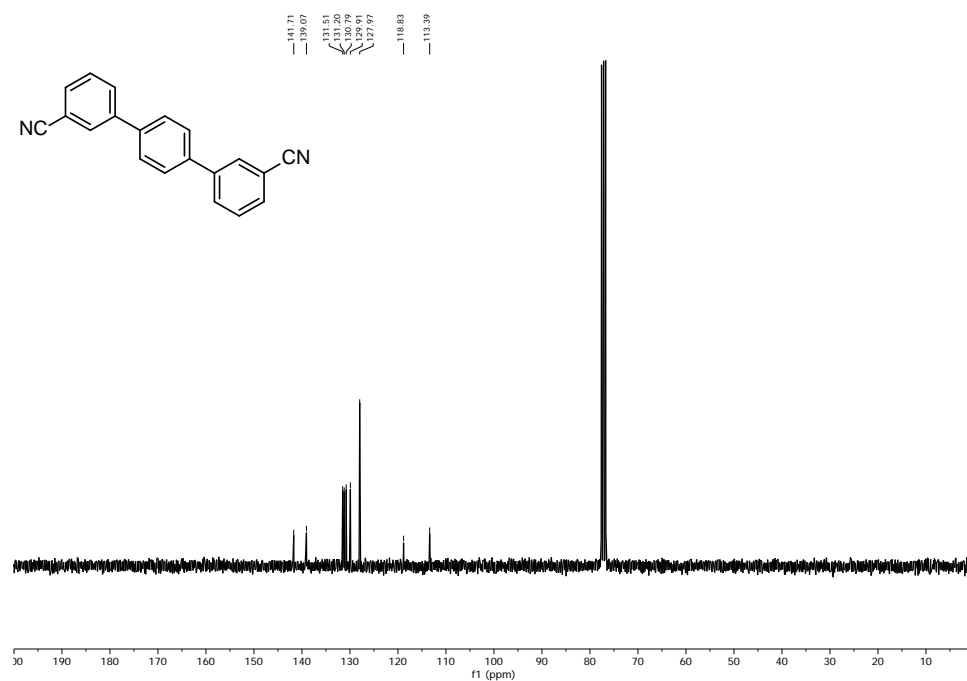
SI-Figure 13. Distance measurement of **DAP** on Au(111) surface and its lineprofile along the molecule ($5.9 \text{ nm} \times 5.9 \text{ nm}$, -0.2 V , 50 pA). The edge-to-edge distance of the diazapyrene group showed here was measured to be 0.66 nm , and the average distance of 10 measurements is $0.65 \pm 0.02 \text{ nm}$. Again, the edge-to-edge distance could be different with different image contrast. The distance here is to show that it is comparable with the *c*-QDN.

3. ^1H - and ^{13}C -NMR spectra of new compounds

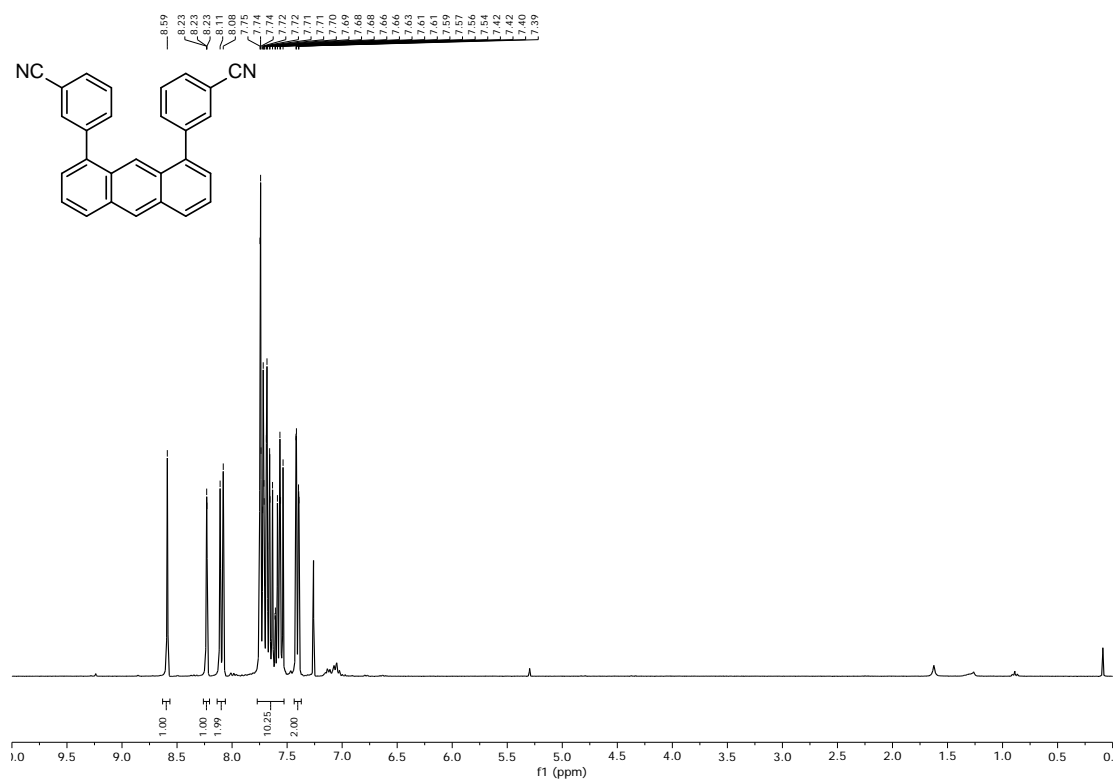
^1H NMR (300 MHz, CDCl_3 , 293 K) of *p*-Terphenyl-3,3''-dicyanitril (**8**)



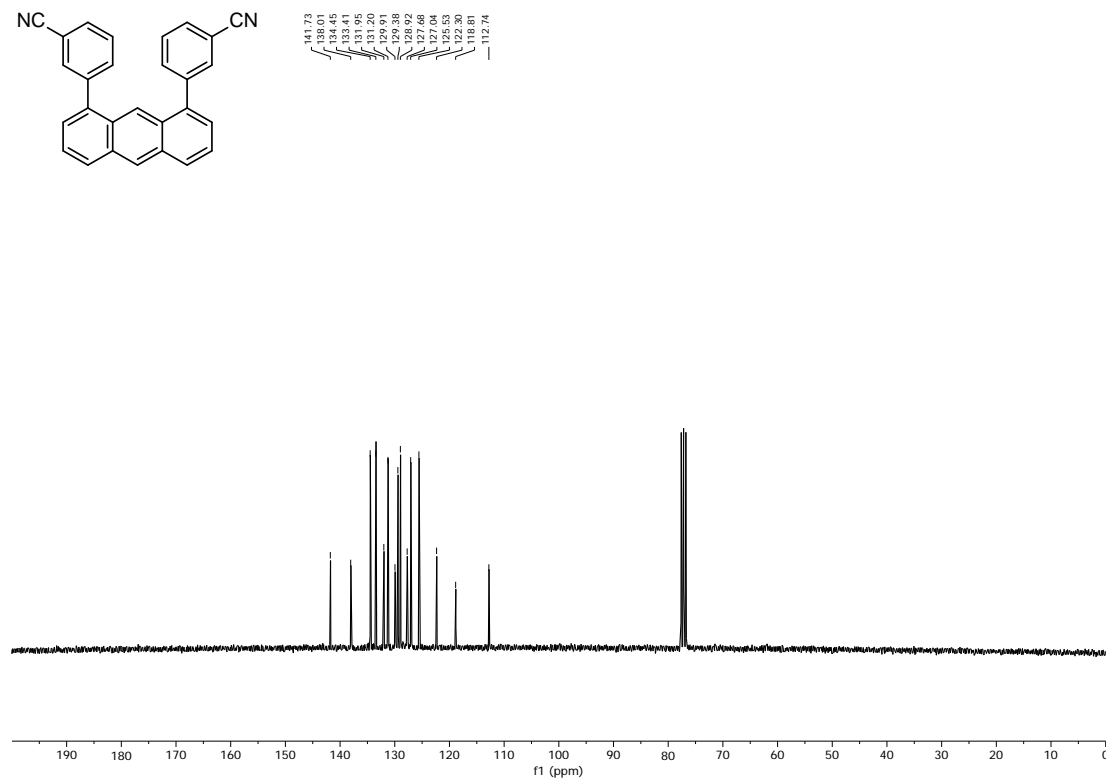
^{13}C NMR (75 MHz, CDCl_3 , 293 K) of *p*-Terphenyl-3,3''-dicyanitril (**8**)



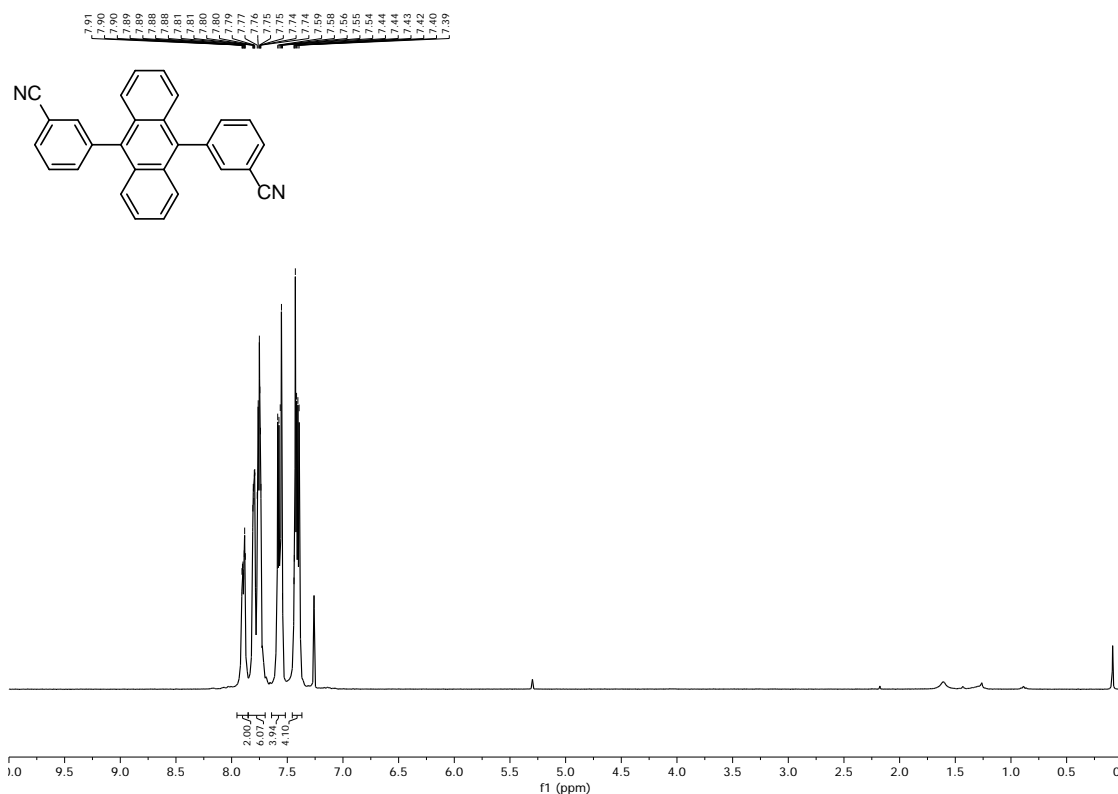
^1H NMR (300 MHz, CDCl_3 , 293 K) of 3,3'-(Anthracene-1,8-diyl)dibenzonitrile (9)



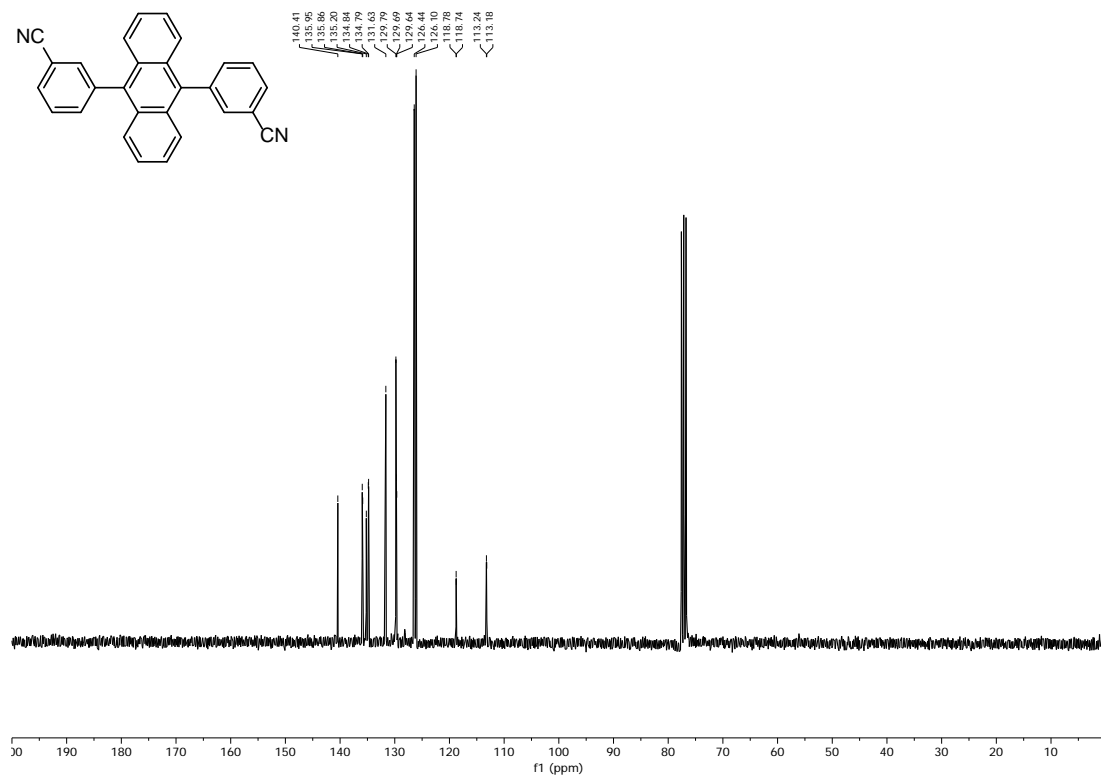
^{13}C NMR (75 MHz, CDCl_3 , 293 K) of 3,3'-(Anthracene-1,8-diyl)dibenzonitrile (9)



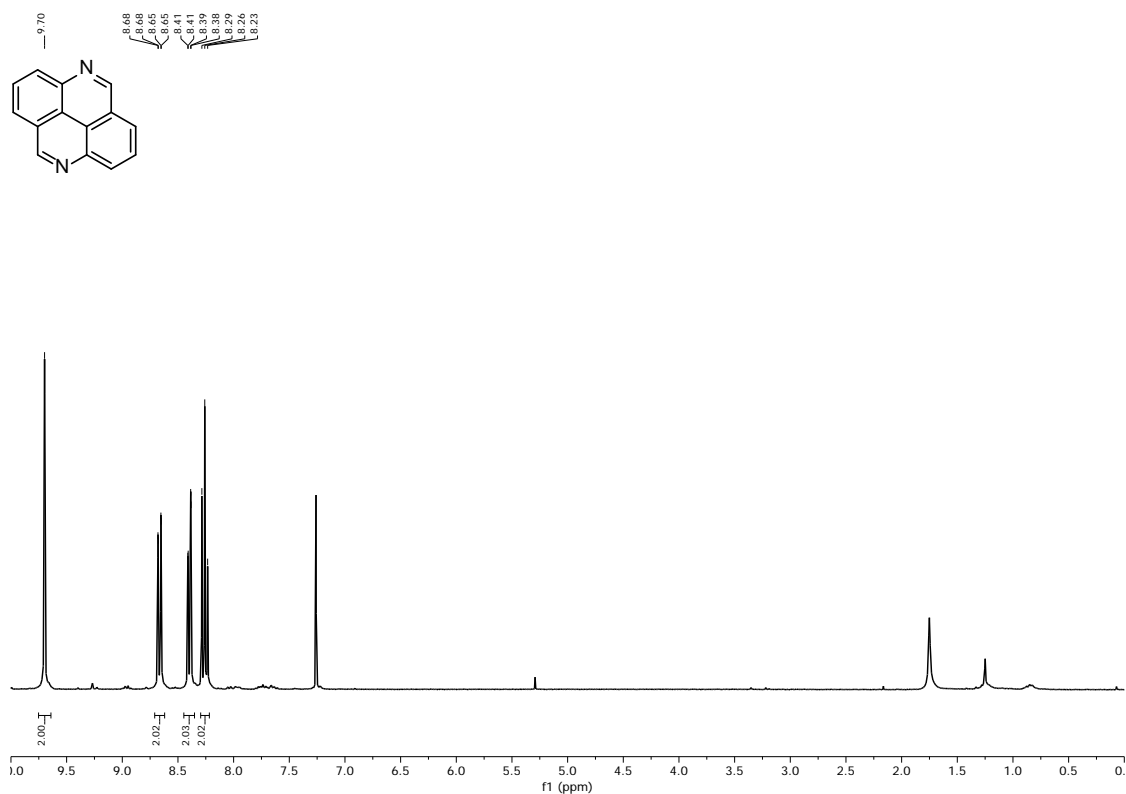
¹H NMR (300 MHz, CDCl₃, 293 K) of 3,3'-(Anthracene-9,10-diyl)dibenzonitrile (10)



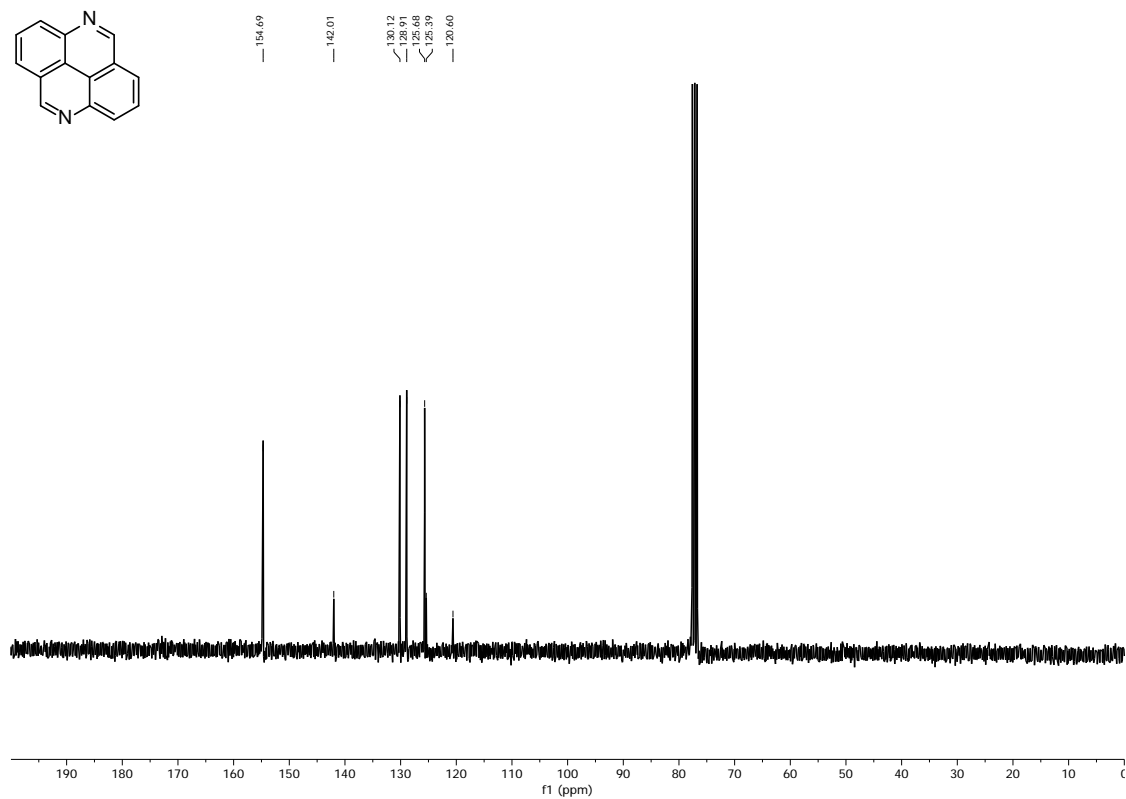
¹³C NMR (75 MHz, CDCl₃, 293 K) of 3,3'-(Anthracene-9,10-diyl)dibenzonitrile (10)



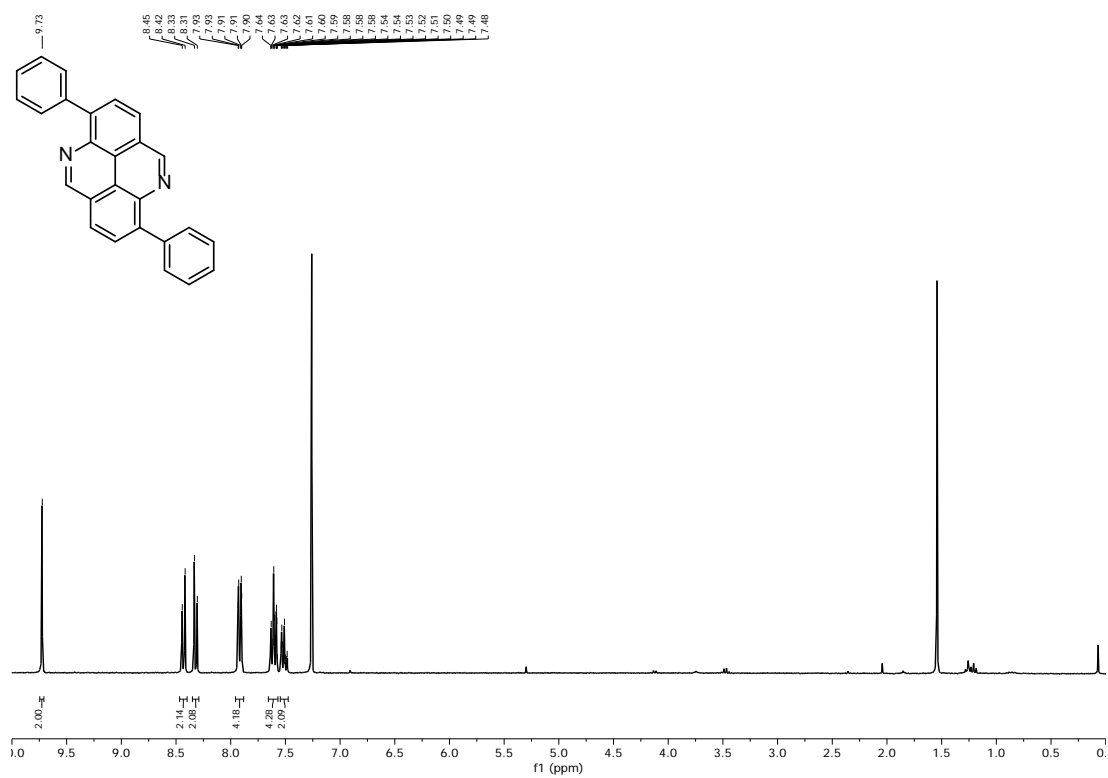
^1H NMR (300 MHz, CDCl_3 , 293 K) of 4,9-Diazapyrene (13)



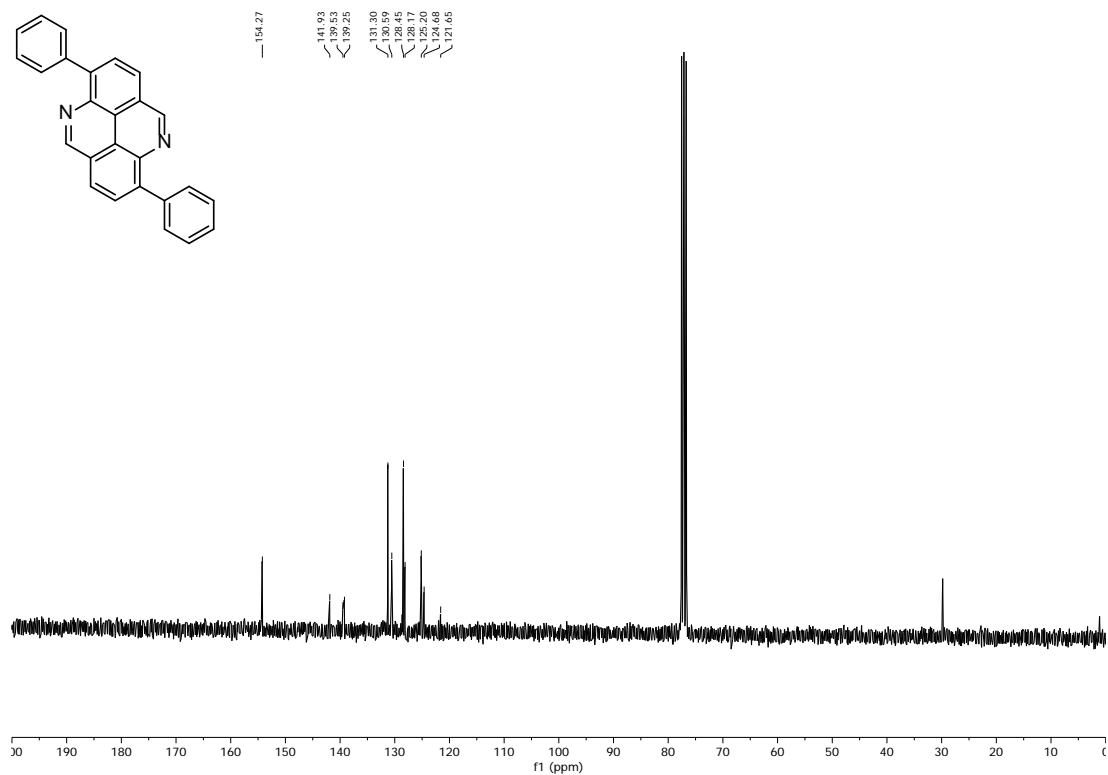
^{13}C NMR (75 MHz, CDCl_3 , 293 K) of 4,9-Diazapyrene (13)



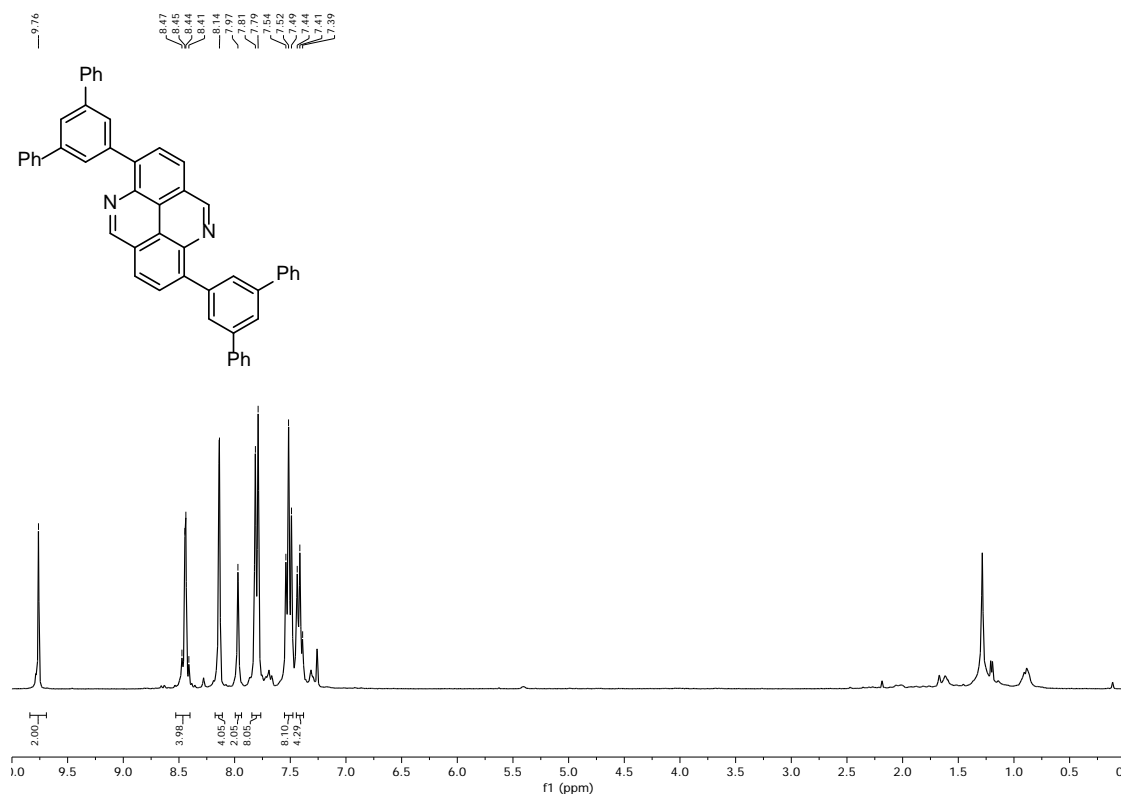
¹H NMR (300 MHz, CDCl₃, 293 K) of 4,9-Diaza-3,8-diphenylpyrene (3)



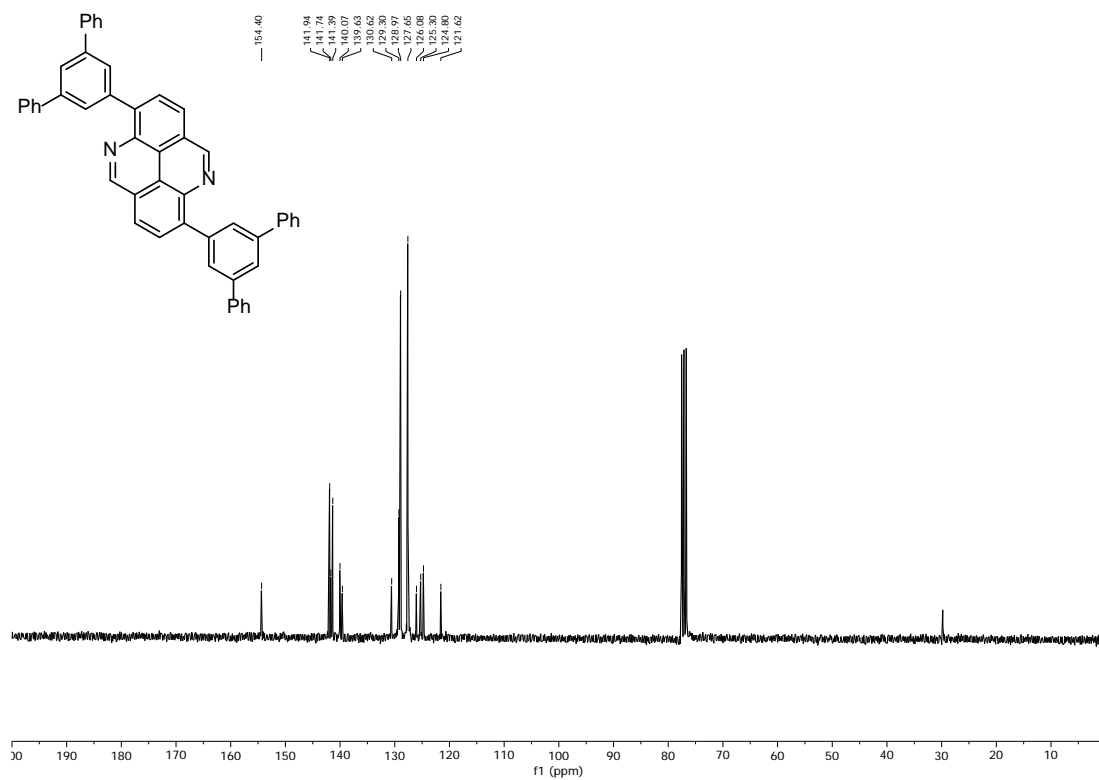
¹³C NMR (75 MHz, CDCl₃, 293 K) of 4,9-Diaza-3,8-diphenylpyrene (3)



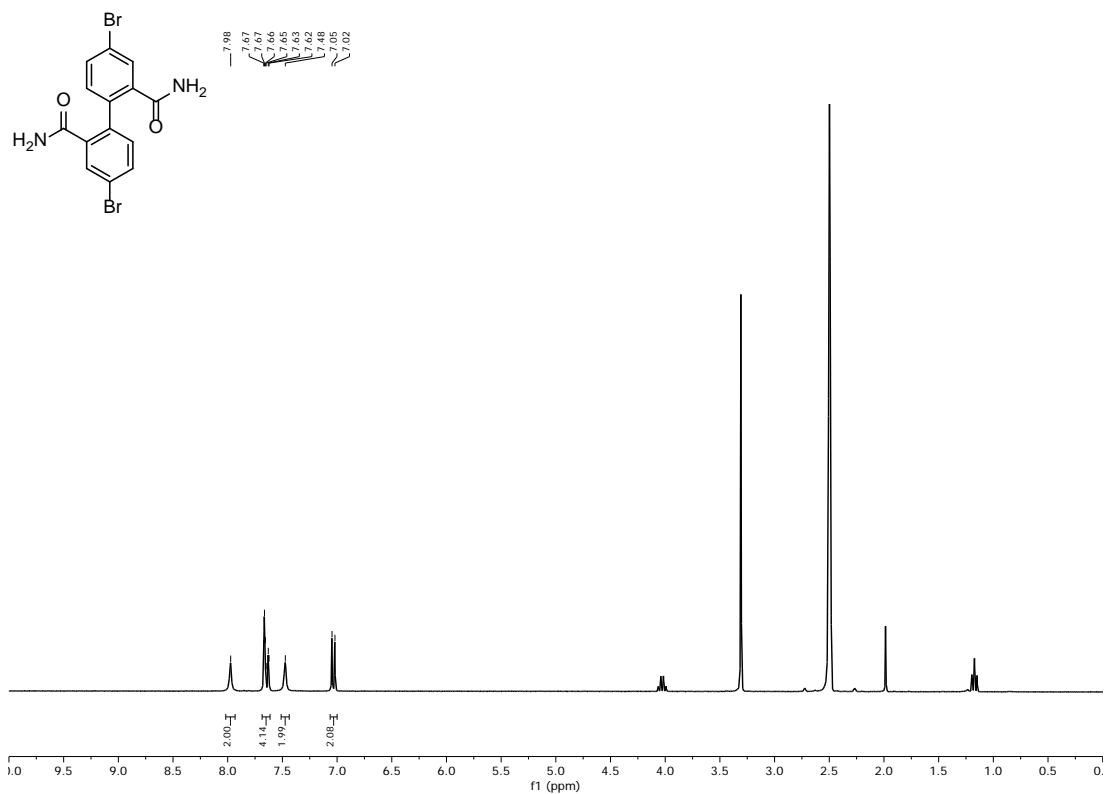
¹H NMR (300 MHz, CDCl₃, 293 K) of 4,9-Diaza-3,8-bis(3,5-phenylphen-1-yl)pyrene (4)



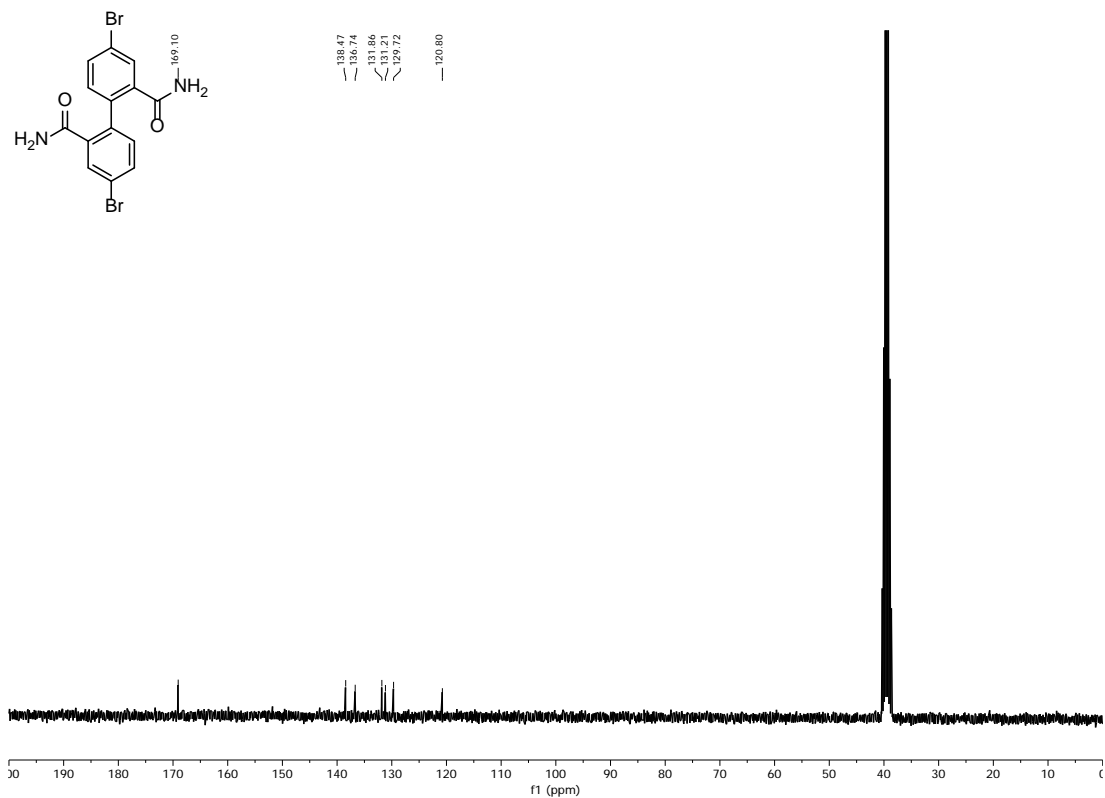
¹³C NMR (75 MHz, CDCl₃, 293 K) of 4,9-Diaza-3,8-bis(3,5-phenylphen-1-yl)pyrene (4)



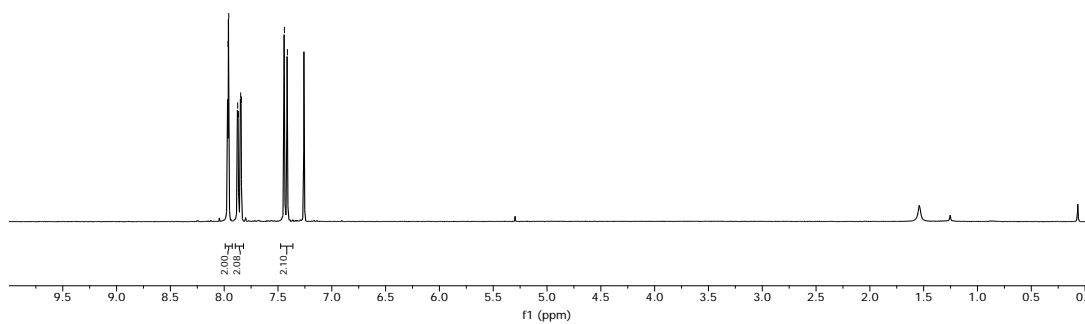
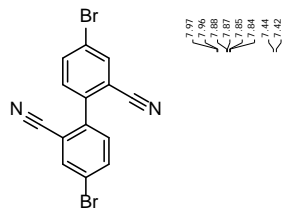
¹H NMR (300 MHz, CDCl₃, 293 K) of 4,4'-Dibromobiphenyl-2,2'-dicarboxamide (15)



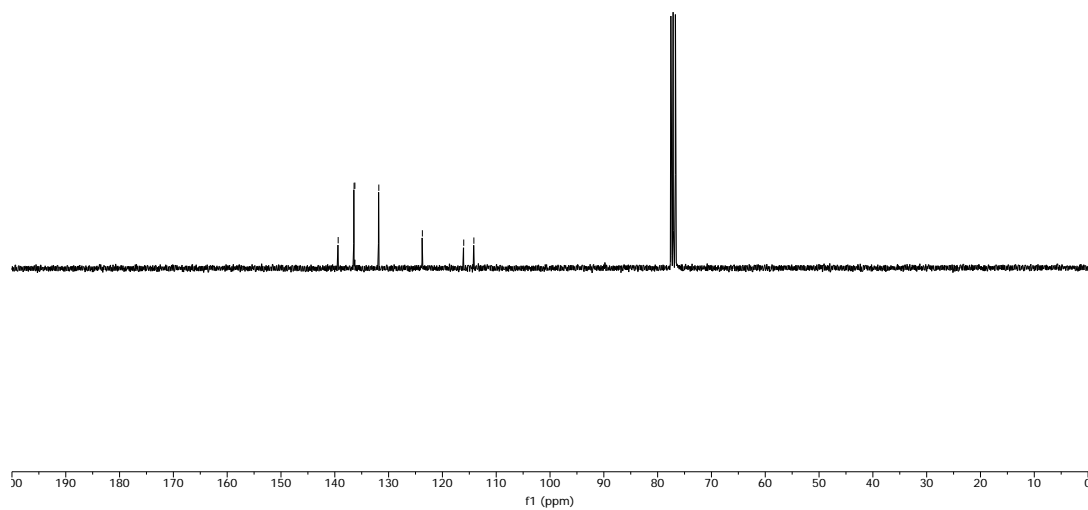
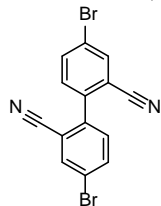
¹³C NMR (75 MHz, CDCl₃, 293 K) of 4,4'-Dibromobiphenyl-2,2'-dicarboxamide (15)



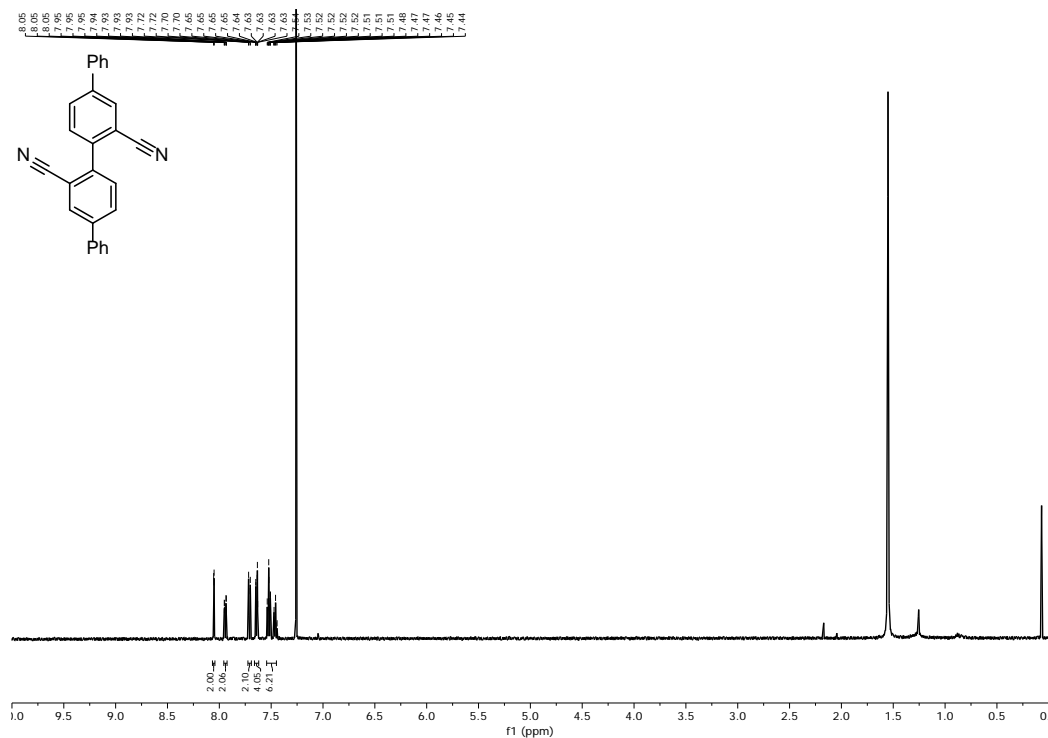
¹H NMR (300 MHz, CDCl₃, 293 K) of 4,4'-Dibromobiphenyl-2,2'-dicarbonitrile (16)



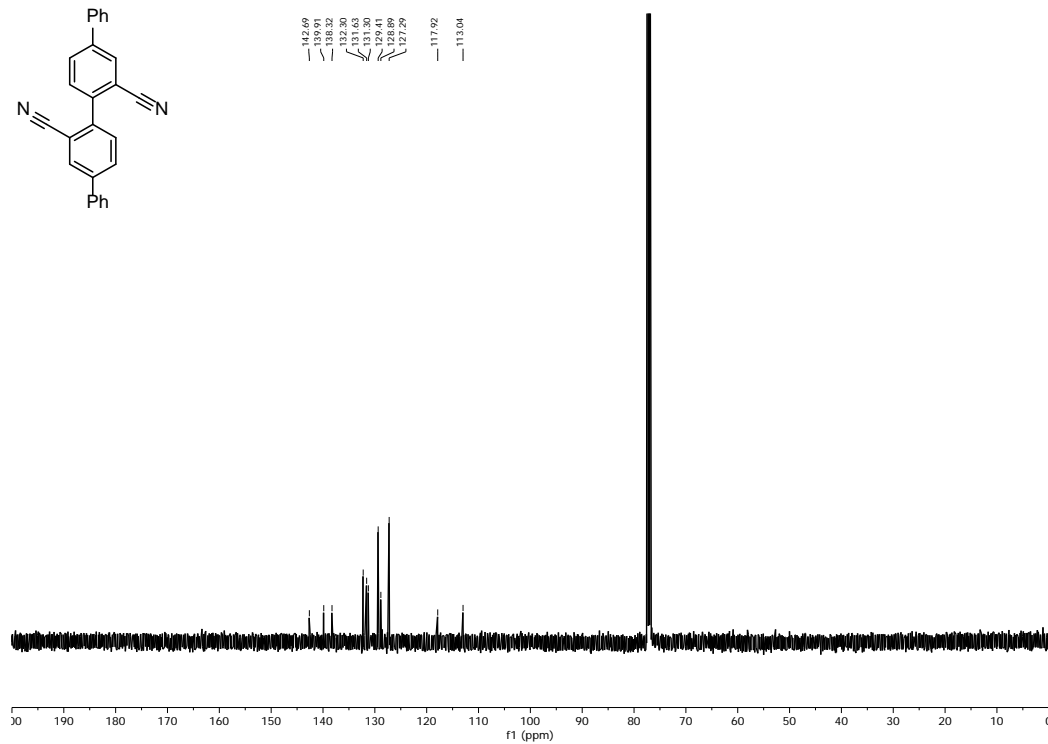
¹³C NMR (75 MHz, CDCl₃, 293 K) of 4,4'-Dibromobiphenyl-2,2'-dicarbonitrile (16)



¹H NMR (500 MHz, CDCl₃, 293 K) of [1,1':4',1'':4'',1''']-Quarterphenyl]-2'',3'-dicyanitrile (5)



¹³C NMR (126 MHz, CDCl₃, 293 K) of [1,1':4',1'':4'',1''']-Quarterphenyl]-2'',3'-dicyanitrile (5)



Literature

- 1 S. Zhao, L. Kang, H. Ge, F. Yang, C. Wang, C. Li, Q. Wang and M. Zhao, *Synth. Commun.*, 2012, **42**, 3569-3578.
- 2 M. Dincă, A. Dailly, C. Tsay and J. R. Long, *Inorg. Chem.*, 2008, **47**, 11-13.
- 3 M. Novi, G. Garbarino, G. Petrillo and C. Dell'Erba, *Tetrahedron*, 1990, **46**, 2205-2212.
- 4 C. C. Scarborough, B. V. Popp, I. A. Guzei and S. S. Stahl, *J. Organomet. Chem.*, 2005, **690**, 6143-6155.
- 5 M. Tobisu, K. Koh, T. Furukawa and N. Chatani, *Angew. Chem. Int. Ed.*, 2012, **51**, 11363-11366.
- 6 B. E. Hoogenboom, O. H. Oldenziel and A. M. van Leusen, *Org. Synth.*, 1977, **7**, 102-106.
- 7 R. F. Robbins, *J. Chem. Soc.*, 1960, 2553-2556.
- 8 J. Kwak, M. Kim and S. Chang, *J. Am. Chem. Soc.*, 2011, **133**, 3780-3783.
- 9 C. D. Bösch, S. M. Langenegger and R. Häner, *Angew. Chem. Int. Ed.*, 2016, **55**, 9961-9964.
- 10 G. Kresse and J. Hafner, *Phys. Rev. B*, 1993, **47**, 558-561.
- 11 G. Kresse and J. Furthmüller, *Comput. Mat. Sci.*, 1996, **6**, 15-50.
- 12 G. Kresse and J. Furthmüller, *Phys. Rev. B*, 1996, **54**, 11169-11186.
- 13 P. E. Blöchl, *Phys. Rev. B*, 1994, **50**, 17953-17979.
- 14 G. Kresse and D. Joubert, *Phys. Rev. B*, 1999, **59**, 1758-1775.
- 15 J. Perdew, K. Burke and M. Ernzerhof, *Phys. Rev. Lett.*, 1996, **77**, 3865.
- 16 J. Perdew, K. Burke and M. Ernzerhof, *Phys. Rev. Lett.*, 1997, **78**, 1396.
- 17 S. Grimme, J. Antony, S. Ehrlich and H. Krieg, *J. Chem. Phys.*, 2010, **132**, 154104.
- 18 S. Grimme, S. Ehrlich and L. Goerigk, *J. Comput. Chem.*, 2011, **32**, 1456.
- 19 A. D. Becke and E. R. Johnson, *J. Chem. Phys.*, 2005, **123**, 154101.
- 20 E. R. Johnson and A. D. Becke, *J. Chem. Phys.*, 2005, **123**, 024101.
- 21 E. R. Johnson and A. D. Becke, *J. Chem. Phys.*, 2006, **124**, 174104.
- 22 C. Kittel, *Introduction to Solid State Physics*, 8th ed., John Wiley & Sons, Inc.: New York, 2005.
- 23 J. Tersoff and D. R. Hamann, *Phys. Rev. Lett.*, 1983, **50**, 1998-2001.
- 24 V. Blum, R. Gehrke, F. Hanke, P. Havu, V. Havu, X. Ren, K. Reuter and M. Scheffler, *Comput. Phys. Commun.*, 2009, **180**, 2175-2196.

- 25 Alexandre Tkatchenko, Alberto Ambrosetti and Robert A. DiStasio Jr., *J. Chem. Phys.*, 2013, **138**, 074106.
- 26 Alexandre Tkatchenko, Robert A. DiStasio Jr., Roberto Car and Matthias Scheffler, *Phys. Rev. Lett.*, 2012 **108**, 236402.
- 27 W. Humphrey, A. Dalke and K. Schulten, *J. Molec. Graphics*, 1996, **14**, 33-38.
- 28 I. Horcas, R. Fernandez, J.M. Gomez-Rodriguez, J. Colchero, J. Gomez-Herrero and A.M. Baro, *Review of Scientific Instruments*, 2007, **78**, 013705.